



Research paper

Design, synthesis, and biological evaluations of novel 3-amino-4-ethynyl indazole derivatives as Bcr-Abl kinase inhibitors with potent cellular antileukemic activity

Ashraf K. El-Damasy^{a, b, **, *}, Heewon Jin^{a, c}, Seon Hee Seo^a, Eun-Kyoung Bang^a, Gyochang Keum^{a, d, *}

^a Center for Neuro-Medicine, Brain Science Institute, Korea Institute of Science and Technology (KIST), Seoul, 02792, Republic of Korea

^b Department of Medicinal Chemistry, Faculty of Pharmacy, Mansoura University, Mansoura, 35516, Egypt

^c Department of Chemistry, College of Natural Sciences, Seoul National University, Seoul, 151-747, Republic of Korea

^d Division of Bio-Medical Science & Technology, KIST School, Korea University of Science and Technology (UST), Seoul, 02792, Republic of Korea

ARTICLE INFO

Article history:

Received 5 June 2020

Received in revised form

29 July 2020

Accepted 30 July 2020

Available online 19 August 2020

Keywords:

3-Aminoindazole

Ethynyl linker

Diarylamide

Bcr-Abl^{WT}

Bcr-Abl^{T315I}

Imatinib resistance

Antileukemic activity

NanoBRET target engagement

ABSTRACT

Breakpoint cluster region-Abelson (Bcr-Abl) kinase is a key driver in the pathophysiology of chronic myelogenous leukemia (CML). Broadening the chemical diversity of Bcr-Abl kinase inhibitors with novel chemical entities possessing favorable target potency and cellular efficacy is a current medical demand for CML treatment. In this respect, a new series of ethynyl bearing 3-aminoindazole based Bcr-Abl inhibitors has been designed, synthesized, and biologically evaluated. The target compounds were designed based on introducing the key structural features of ponatinib, alkyne spacer and diarylamide, into the previously reported indazole **II** to improve its Bcr-Abl inhibitory activity and overcome its poor cellular potency. All target compounds elicited potent activity against Bcr-Abl^{WT} with sub-micromolar IC₅₀ values ranging 4.6–667 nM. In addition, certain derivatives exhibited promising potency over the clinically imatinib-resistant Bcr-Abl^{T315I}. Among the target molecules, compounds **9c**, **9h** and **10c** stood as the most potent derivatives with IC₅₀ values of 15.4 nM, 4.6 nM, and 25.8 nM, respectively, against Bcr-Abl^{WT}. Interestingly, **9h** showed 2 folds and 3.6 times superior potency to the lead indazole **II** and **10c**, respectively, against Bcr-Abl^{T315I}. Molecular docking of **9h** pointed out its possibility to be a type II kinase inhibitor. Furthermore, all compounds, except **9b**, showed highly potent antiproliferative activity against the Bcr-Abl positive leukemia K562 cell (MTT assay) surpassing the modest activity of lead indazole **II**. Moreover, the most potent members **9h** and **10c** exerted potent antileukemic activity against NCI leukemia panel, particularly K562 cell (SRB assay) with GI₅₀ less than 10 nM, being superior to the FDA approved drug imatinib. Further biochemical hERG and cellular toxicity, phosphorylation assay, and NanoBRET target engagement of **9h** underscored its merits as a promising candidate for CML therapy.

© 2020 Elsevier Masson SAS. All rights reserved.

1. Introduction

Chronic myelogenous leukemia (CML) is a hematological cancer characterized by uncontrolled growth of myeloid cells [1]. A hallmark of CML is the appearance of a Philadelphia (Ph) chromosome,

which results from reciprocal translocation between the Abelson (ABL) gene on chromosome 9 and the break-point cluster region (Bcr) gene on chromosome 22 [2,3]. This chimeric Bcr-Abl gene encodes the generation of Bcr-Abl fusion protein, a constitutively active tyrosine kinase which triggers the unchecked myeloid cell proliferation [4]. Therefore, the development of Bcr-Abl kinase inhibitors has been emerged as a legitimate approach for CML therapy.

Imatinib (STI-571, Fig. 1), a pyridopyrimidine inhibitor of Bcr-Abl, was approved by FDA in 2001 for the treatment of CML [5,6]. Crystal structures of imatinib-Bcr-Abl complex revealed that imatinib is a type II kinase inhibitor, which binds to the ATP binding site

* Corresponding author. Center for Neuro-Medicine, Brain Science Institute, Korea Institute of Science and Technology (KIST), Seoul, 02792, Republic of Korea.

** Corresponding author. Department of Medicinal Chemistry, Faculty of Pharmacy, Mansoura University, Mansoura 35516, Egypt.

E-mail addresses: ashraf.el-damasy@kist.re.kr, ph_karem2000@mans.edu.eg (A.K. El-Damasy), gkeum@kist.re.kr (G. Keum).

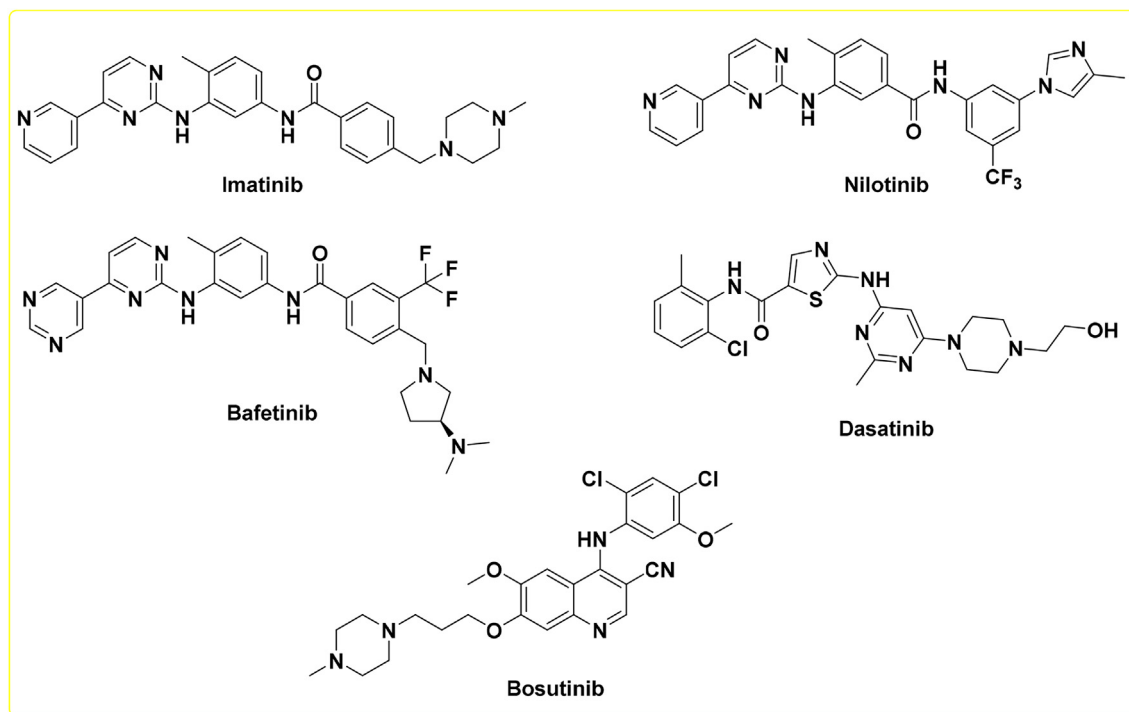


Fig. 1. Chemical structures of representative first and second generation Bcr-Abl kinase inhibitors.

as well as to a hydrophobic allosteric pocket that was only exposed upon flipping out of the conserved DFG motif [7,8]. Despite the initial therapeutic benefits of imatinib, the emergence of point mutations within the Abl kinase domain hampered imatinib efficacy in many patients with advanced phases of CML [9,10]. The gatekeeper T315I mutation in Bcr-Abl accounts for approximately 20% of all clinically relevant CML mutations [11,12]. T315I mutation represents a major pitfall for design of Bcr-Abl inhibitors, as it can change the geometry of the ATP-binding pocket to hinder several essential protein–ligand interaction sites and eliminate a crucial hydrogen bond needed for tight binding of the inhibitors [13]. A number of second-generation Bcr-Abl kinase inhibitors like nilotinib [14], bafetinib [15], dasatinib [16], and bosutinib [17] (Fig. 1) have been developed to circumvent the imatinib resistance in CML. Nevertheless, these drugs are effective against most of imatinib-resistant forms of Bcr-Abl excluding the gatekeeper T315I mutation.

Recently, several Bcr-Abl inhibitors capable of inhibiting both native Bcr-Abl and its clinically resistant T315I mutant were identified [18–22]. Among them, ponatinib (AP24534, Fig. 2) [20,23] was of special interest. Ponatinib contains an ethynyl linker bridging its hinge binding motif, imidazo[1,2-*b*]pyridazine, with the diarylamide side chain [20]. The slim acetylene spacer contributed to the success of ponatinib by avoiding steric clash with a bulky isoleucine residue at the gatekeeper region [24]. Also, the terminal substituted 3-trifluoromethylphenyl appendage served as an allosteric site binding moiety for optimum Bcr-Abl inhibitory activity. Further structural modifications of ponatinib were conducted applying scaffold hopping approach for variation of the imidazo[1,2-*b*]pyridazine head, while conserving the other key structural features (the ethynyl bridge and diarylamide fragment) [22,25]. Such endeavors resulted in identification of equipotent ponatinib congeners with different heterocycle scaffolds, GZD824 [22] and pyrazolopyrimidine derivative (I) [25] (Fig. 2). Accordingly, it could be emphasized that tethering appropriate hinge binding head to the proper diarylamide fragment through alkyne bridge would

generate diverse new chemical entities as potent Bcr-Abl kinase inhibitors.

On the other hand, 3-aminoindazole represents one of the substantial hinge binding motifs, which was exploited for development of several kinase inhibitors as anticancer agents. Linifanib (ABT-869), is one of the earlier 3-aminoindazole members, which was identified as an orally active multikinase inhibitor (KDR, FLT3 and c-KIT) with considerable antitumor activity in various pre-clinical animal xenograft models [26]. Its privileged 3-aminoindazole was further utilized as a hinge binder in a number of small molecules targeting various oncogenic kinases, including Aurora B [27], VEGFR2 [28,29], c-Met [30]. Interestingly, Shan *et al.* reported a series of aminoindazole based Bcr-Abl inhibitors [31]. Few derivatives of this series, particularly the most active member II (Fig. 3), elicited reasonable Bcr-Abl inhibitory activity, however with modest cellular antileukemic activity over the Bcr-Abl dependent K562 cell line ($GI_{50} = 6500$ nM) [31], which might need further optimization. In view of the success of ponatinib and its analogues in inhibiting both Bcr-Abl^{WT} and Bcr-Abl^{T315I} with remarkable cellular potency, we hypothesized that incorporation of the key structural domains of ponatinib into the lead indazole II would generate new chemotypes of Bcr-Abl inhibitors with improved activity (Fig. 3). In this regard, a multidimensional campaign of structural modifications based on II was performed (Fig. 3). An ethynyl linker was introduced to tether both indazole and diarylamide moieties, and amide or reversed amide was utilized to bridge the central and terminal phenyl rings instead of the dicarbonylpiperazine in II. In addition, the terminal dichlorophenyl ring of II was modified to various substituted 3-trifluoromethylphenyl derivatives in attempt to achieve better Bcr-Abl inhibitory and cellular potencies.

In terms of the binding interactions with Bcr-Abl kinase, new ethynyl-containing indazoles were designed so that the 3-aminoindazole could serve as a hinge binding motif with Met318 and Glu316 residues. In addition, the ethynyl linker would allow the

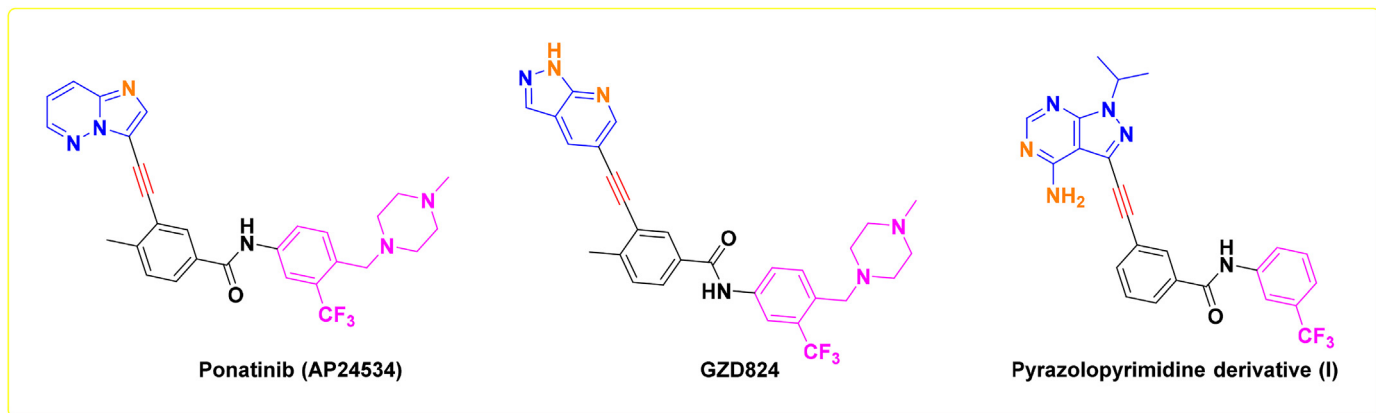


Fig. 2. Chemical structures of ponatinib and alkyne containing Bcr-Abl kinase inhibitors. The blue color refers to the head motif, and the orange colored nitrogen atoms are involved in binding interactions with hinge region. (For interpretation of the references to color in this figure legend, the reader is referred to the Web version of this article.)

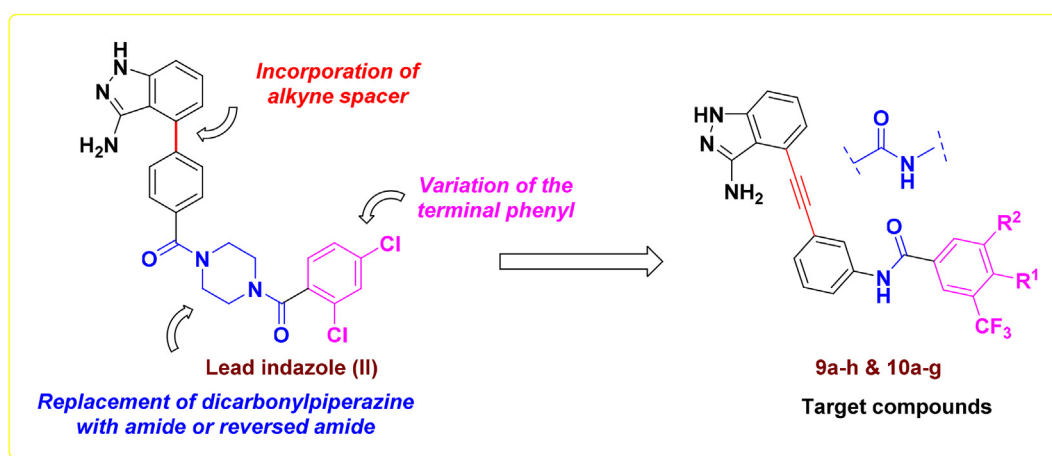


Fig. 3. Rational design of the target compounds.

compound to traverse the gatekeeper T315 and bypass its corresponding bulky I315. Moreover, the terminal substituted-trifluoromethyl ring could efficiently approach the hydrophobic allosteric pocket of Bcr-Abl kinase domain (Fig. 4). To the best of our

knowledge, this set of structural modifications for compound II has not been investigated before for its Bcr-Abl inhibitory activity. In view of the aforementioned considerations, and in continuation to our ongoing efforts to identify new potent kinase inhibitors [32,33],

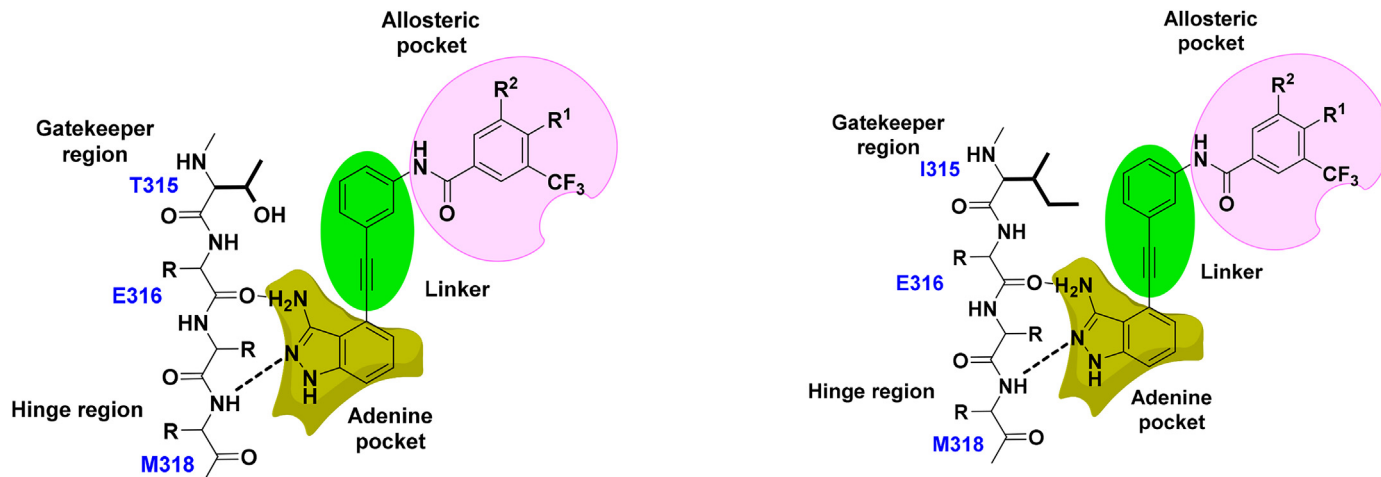


Fig. 4. Schematic representations illustrating the putative binding of the designed compounds with Bcr-Abl^{WT} (left panel) and Bcr-Abl^{T315I} (right panel) kinase.

we herein report for the first time a new series of ethynyl containing indazoles as potent Bcr-Abl kinase inhibitors.

2. Results and discussion

2.1. Chemistry

In order to prepare the target compounds, the key intermediate acetylenes **2a–h** and **7a–g** were synthesized from 3-ethynylaniline **1** and 3-ethynylbenzoic acid **6**, respectively, as shown in Scheme 1. Treatment of 3-ethynylaniline **1** with acid chloride in either Et₃N/DCM at room temperature or pyridine at 90 °C afforded the diarylbenzamides **2a** and **2b**, respectively. Compounds **2c–h** were obtained through coupling of **1** with different carboxylic acids using 2-(7-aza-1H-benzotriazole-1-yl)-1,1,3,3-tetramethyluronium hexafluorophosphate (HATU) as a coupling agent and DIPEA as a base in anhydrous DMF. Esterification of 3-iodobenzoic acid **3** with methanol, followed by silylation with trimethylsilylacetylene (TMS) produced the silylated ester **5**. Subsequent desilylation and alkaline hydrolysis of **5** generated 3-ethynylbenzoic acid **6**. Amide coupling of **6** with different anilines was accomplished adopting the same conditions for compounds **2c–h**, however at 60 °C, to furnish the reversed amides **7a–g**.

The diarylamide containing indazoles **9a–h** and **10a–g** were synthesized as depicted in Scheme 2. Cyclization of 2-fluoro-6-iodobenzonitrile with hydrazine hydrate in *n*-butanol afforded the 4-iodoindazol-3-yl amine **8** [26] as the main building block for the target compounds. Sonogashira coupling of **8** with the proper acetylene derivatives **2a–h** or **7a–g** was performed utilizing PdCl₂(PPh₃)₂ and CuI as catalysts in Et₃N/DMF (1:1) at 90 °C under argon atmosphere to provide the desired final compounds **9a–h** and **10a–g**.

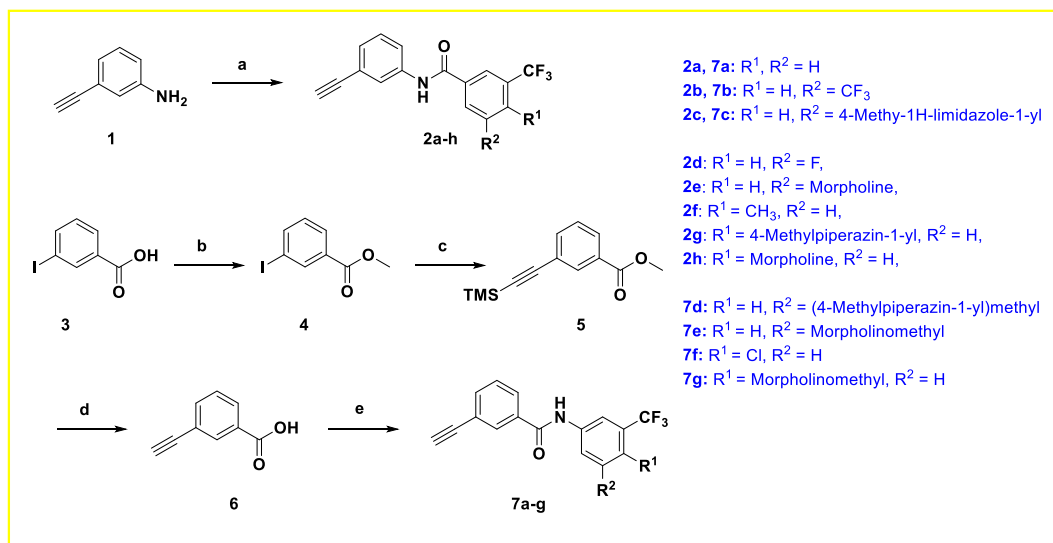
2.2. In vitro biochemical kinase screening

2.2.1. Bcr-Abl^{WT} and Bcr-Abl^{T315I} kinase evaluations

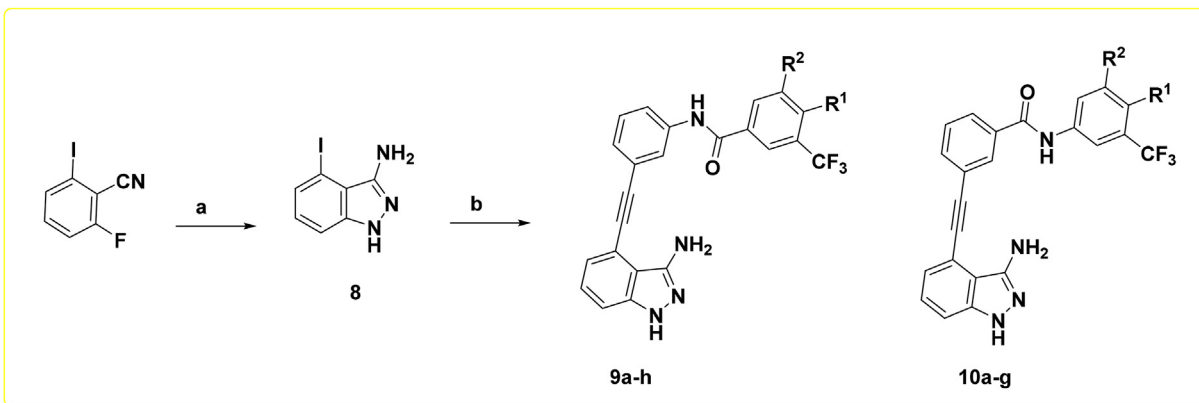
All final compounds were tested to determine their IC₅₀ values against both the native Bcr-Abl^{WT} and its imatinib-resistant mutant Bcr-Abl^{T315I} at Reaction Biology Corporation (RBC, Malvern, PA, USA) [34], using imatinib as a reference compound and

staurosporine, a pan kinase inhibitor, as a positive control (Table 1). As revealed from the data, all compounds elicited potent activity against Bcr-Abl^{WT} with sub-micromolar IC₅₀ values spanning in the range of 4.6–667 nM. In addition, certain derivatives displayed promising potency towards Bcr-Abl^{T315I} with IC₅₀ values of 227–2550 nM. Upon inspection of the activity of amides **9a–c** and their corresponding reversed amides **10a–c**, it is noted that reversed amide linker is relatively more favorable for Bcr-Abl^{WT} inhibitory activity. For example, 3,5-bis-trifluoromethyl derivative **10b** with reversed amide spacer showed superior activity (Bcr-Abl^{WT} IC₅₀ = 0.186 μM, Bcr-Abl^{T315I} IC₅₀ = 1.480 μM) than its amide congener **9b** (Bcr-Abl^{WT} IC₅₀ = 0.667 μM, Bcr-Abl^{T315I} IC₅₀ > 20.0 μM).

Concerning the activity of amide derivatives **9a–h**, it was found that introduction of additional trifluoromethyl group, as in **9b**, at *meta* position of 3-trifluoromethyl derivative **9a** led to two times drop in Bcr-Abl^{WT} activity (**9b**, Bcr-Abl^{WT} IC₅₀ = 0.667 μM; **9a**, Bcr-Abl^{WT} IC₅₀ = 0.313 μM) and dramatic loss of activity towards Bcr-Abl^{T315I} (**9b**, Bcr-Abl^{T315I} IC₅₀ > 20.0 μM). In contrast, replacing *m*-trifluoromethyl group in **9b** with fluorine **9d** significantly improved the Bcr-Abl^{WT} inhibitory activity (**9d**, Bcr-Abl^{WT} IC₅₀ = 0.172 μM). Similarly, the methyl derivative **9f** (Bcr-Abl^{WT} IC₅₀ = 0.104 μM) was of promising activity, which may point out that incorporation of small lipophilic group like fluorine or methyl at *meta* or *ortho* position of **9a** is tolerable for Bcr-Abl^{WT} inhibitory activity. Intriguingly, insertion of hydrophilic 4-methylimidazole **9c** or morpholine **9h** at *meta* or *ortho* position of **9a**, respectively, resulted in substantial improvement of activity (**9c**, Bcr-Abl^{WT} IC₅₀ = 0.0154 μM, Bcr-Abl^{T315I} IC₅₀ = 1.44 μM; **9h**, Bcr-Abl^{WT} IC₅₀ = 0.0046 μM, Bcr-Abl^{T315I} IC₅₀ = 0.227 μM). Unexpectedly, shifting the morpholine moiety of **9h** from *ortho* to *meta* position, **9e**, was deleterious for activity (**9e**, Bcr-Abl^{WT} IC₅₀ = 0.637 μM, Bcr-Abl^{T315I} IC₅₀ = 4.84 μM). Moreover, replacing morpholine in **9h** with 4-methylpiperazine **9g** was associated with 33 folds drop in activity (**9g**, Bcr-Abl^{WT} IC₅₀ = 0.151 μM). Such biochemical outcomes indicate that the Bcr-Abl inhibitory activity of target compounds is greatly modulated by the substitution pattern (nature and position) of 3-trifluoromethylphenyl ring as the allosteric pocket binding domain. Furthermore, it could be concluded that installing hydrophilic moieties (morpholine and methyl-imidazole) neighboring to



Scheme 1. Reaction conditions and yields **a**) For **2a**; acid chloride, Et₃N, DCM, rt, 2 h, 54.4%, for **2b**; acid chloride, pyridine, 90 °C, 1 h, 53%, for **2c–h**; appropriate carboxylic acid, HATU, DIPEA, DMF, rt, 18 h, 41.8–97.2%; **b**) MeOH, conc. H₂SO₄ (cata.), reflux, 2.5 h, 99%; **c**) Trimethylsilylacetylene, PdCl₂(PPh₃)₂, CuI, Et₃N, THF, rt, 18 h, 96%; **d**) i) 2 N Aq. NaOH, 0 °C, MeOH, 0 °C to rt, 1 h, ii) 2 N Aq. HCl, 84.3%; **e**) Appropriate aniline, HATU, DIPEA, DMF, 60 °C, 4 h, 23.8–73.6%.



Scheme 2. Reaction conditions and yields a) NH₂NH₂·H₂O, n-BuOH, 110 °C, 2 h, 98%; b) 2a–h or 7a–g, PdCl₂(PPh₃)₂, CuI, Et₃N/DMF (1:1), 90 °C, 18 h, 11–76.2%.

trifluoromethyl group of distal phenyl is advantageous than lipophilic groups (methyl and trifluoromethyl) for achieving optimal Bcr-Abl inhibitory activity. This might be attributed to the orientation of the introduced hydrophilic fragments to a solvent-exposed region close to the allosteric pocket, which consequently improves the inhibitor's binding affinity with Bcr-Abl kinase.

Referring to the activity of reversed amides **10a–g**, it was found that insertion of lipophilic trifluoromethyl (**10b**) or chlorine (**10f**) on 3-trifluoromethylphenyl derivative **10a** had a marginal impact on both Bcr-Abl^{WT} and Bcr-Abl^{T315I} inhibitory activity. For instance, compound **10f** exhibited IC₅₀ values of 0.255 μM and 1.420 μM over Bcr-Abl^{WT} and Bcr-Abl^{T315I}, respectively. On the other hand, compounds **10c**, and **10d** with water solubilizing groups at *meta* position of **10a** manifested the best activity in this series. For example, the imidazole derivative **10c** (Bcr-Abl^{WT} IC₅₀ = 0.0258 μM) is 8 times more potent than 3-trifluoromethylphenyl analog **10a** (Bcr-Abl^{WT} IC₅₀ = 0.210 μM). Similar to amide series, compound **10g** with morpholinomethyl group at *ortho* position to 3-trifluoromethylphenyl ring (Bcr-Abl^{WT} IC₅₀ = 0.1945 μM, Bcr-Abl^{T315I} IC₅₀ = 1.605 μM) manifested superior potency to its positional isomer **10e** (Bcr-Abl^{WT} IC₅₀ = 0.571 μM, Bcr-Abl^{T315I} IC₅₀ = 2.510 μM). Interestingly, compounds **9c**, **9d**, **9f–h**, **10c** and **10d** outperformed imatinib activity against both Bcr-Abl^{WT} and Bcr-Abl^{T315I} kinases. Upon comparison with the reported indazole lead **II**, the morpholine amide **9h** elicited superior potency towards Bcr-Abl^{WT} and Bcr-Abl^{T315I} than compound **II**. Overall, both amide **9h** (Bcr-Abl^{WT} IC₅₀ = 4.6 nM, Bcr-Abl^{T315I} IC₅₀ = 227 nM) and reversed amide **10c** (Bcr-Abl^{WT} IC₅₀ = 25.8 nM, Bcr-Abl^{T315I} IC₅₀ = 824 nM) arise as the most potent members in this series of 3-aminoindazoles. Further structural amendments of **9h** are currently underway to achieve optimal potency towards Bcr-Abl^{T315I} and other clinically relevant mutants.

2.2.2. Kinase profile of 9h

Furthermore, in order to get insights about the kinase selectivity of this novel set of indazoles, the most potent candidate **9h** was tested, at 1 μM concentration, over a panel of 20 oncogenic kinases. As shown in Fig. 5, compound **9h** has elicited considerable inhibitory activity against four kinases; BRAF, c-Src, FLT3 and FMS with % inhibition of 87.75–100. Meanwhile, compound **9h** displayed moderate inhibitory effects (% inhibition = 43.36–65.50) over Aurora A, c-Met, and EGFR kinases, and exerted modest activity against the other examined kinases with % inhibitions < 30.

In view of the obtained outcomes, **9h** was further tested for determination of its IC₅₀ over BRAF, c-Src, FLT3 and FMS kinases (Table 2). Compound **9h** showed IC₅₀ value of 66 nM against c-Src, a

closely related kinase domain of Bcr-Abl, being 14.3 folds more selective for Bcr-Abl^{WT}. Of great significance, compound **9h** elicited exceptional selectivity towards FMS (IC₅₀ = 16.2 nM) over its highly homologous FLT3 kinase (IC₅₀ = 535 nM). Since FMS and FLT3 are key drivers in the pathogenesis of hematopoietic malignancies, particularly acute myeloid leukemia (AML) and acute lymphocytic leukemia (ALL) [35,36], **9h** might have beneficial therapeutic effects for treatment of AML and ALL, beside its activity against CML. In terms of differential activity, the amide member **9h** displayed 3.5 and 26.5 folds selectivity for Bcr-Abl^{WT} over FMS and RAF kinases, respectively.

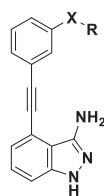
2.3. In vitro cell-based evaluations of the antileukemic activities

2.3.1. Appraisal of the antiproliferative activity by MTT assay

Encouraged by the findings of cell free assay, we investigated the antiproliferative activity of target compounds against the Bcr-Abl positive leukemia K562 cells using MTT method (Table 3). The majority of the tested compounds displayed moderate to potent growth inhibitory activities. In agreement with the obtained biochemical data, the most active three compounds **9c**, **9h** and **10c** exerted the best cellular activity with GI₅₀ values less than 160 nM. Furthermore, amide compounds **9c** and **9h**, as well as reversed amides **10b–d** and **10g** exerted superior cellular potencies to imatinib (GI₅₀ = 0.80 ± 0.14 μM). Compounds **9c** and **10c** possessing 4-methylimidazole moiety exhibited GI₅₀ values of 0.07 ± 0.05 μM and 0.15 ± 0.04 μM, respectively. The amide **9h** (GI₅₀ = 0.02 ± 0.02 μM) with 4-morpholine motif was found to be the best member in this set of compounds. These findings may reveal that the potent antiproliferative effects of those compounds are derived mainly *via* inhibition of Bcr-Abl kinase. Next in the cellular activity order are the reversed amides **10d** (GI₅₀ = 0.30 ± 0.05 μM) and **10g** (GI₅₀ = 0.57 ± 0.19 μM). As disclosed from the results, the presence of proper hydrophilic moiety such as morpholine or 4-methylpiperazine on the terminal 3-trifluoromethylphenyl ring may contribute in significant improvement of compounds' physicochemical properties, water solubility, and hence the cellular potency. While comparing **9h** (GI₅₀ = 0.02 ± 0.02 μM) and **9e** (GI₅₀ = 2.21 ± 0.43 μM), it was noted that shifting the morpholine moiety from *ortho* to *meta* position of 3-trifluoromethylphenyl ring is unfavorable for antileukemic activity. The same conclusion is applicable for compounds **10g** and **10e**.

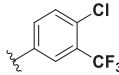
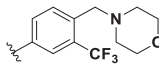
While inspecting the activity of disubstituted derivatives lacking water solubilizing groups **9b**, **9d**, and **9f**, it was found that incorporation of lipophilic trifluoromethyl, fluorine, or methyl at either

Table 1
In vitro kinase inhibitory activity (IC_{50} , μM)^a of the target compounds against Bcr-Abl^{WT} and Bcr-Abl^{T315I}.



Compound No.	X	R	IC_{50} (μM)	
			Bcr-Abl ^{WT}	Bcr-Abl ^{T315I}
9a			0.313	2550
9b			0.667	>20
9c			0.0154 ± 0.002	1.44 ± 0.15
9d			0.172	5.280
9e			0.637	4.840
9f			0.104	2.960
9g			0.151	1.120
9h			0.0046 ± 0.0006	0.227 ± 0.044
10a			0.210	2.260
10b			0.186	1.480
10c			0.0258 ± 0.010	0.824 ± 0.237
10d			0.0567 ± 0.004	1.635 ± 0.485
10e			0.571	2.510

Table 1 (continued)

Compound No.	X	R	IC ₅₀ (μM)	
			Bcr-Abl ^{WT}	Bcr-Abl ^{T315I}
10f			0.255	1.420
10g			0.1945 ± 0.092	1.605 ± 0.245
Imatinib			0.176 ± 0.0175	>100.0
Staurosporine			0.0787	0.0557
Indazole II^b			0.014	0.450

^a All compounds were tested in a 10-dose singlicate or duplicate IC₅₀ mode with 3-fold serial dilution starting at 20 μM, and the reactions were carried out at 10 μM ATP. Bold figures refer to the most potent members.

^b Reported data [31].

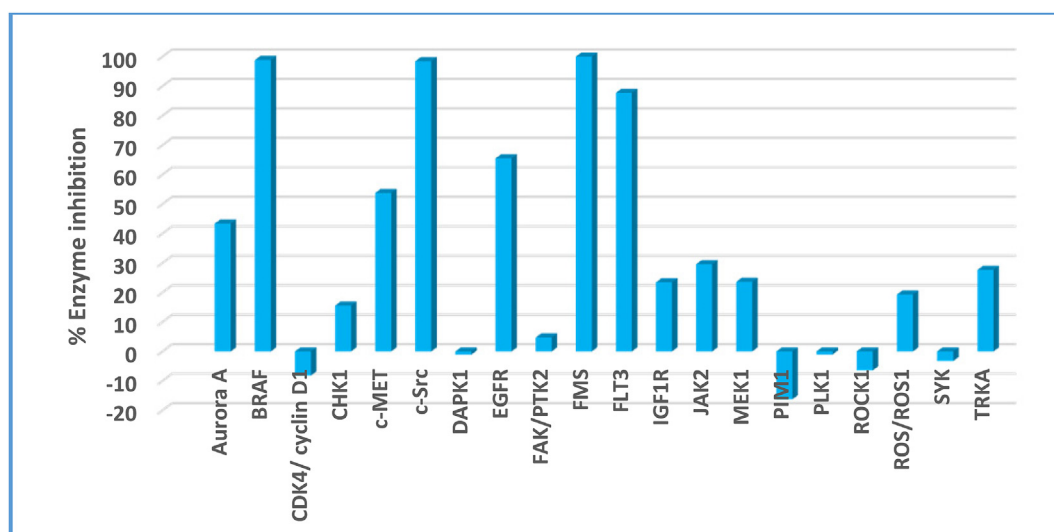


Fig. 5. % Enzyme inhibition (relative to DMSO controls) of compound **9h** (1 μM) against a 20-kinase panel.

Table 2

IC₅₀ of **9h** over BRAF, c-Src, FLT3 and FMS kinases.

Compound No.	IC ₅₀ (μM) ^a			
	BRAF	c-Src	FLT3	FMS
9h	0.122 ± 0.0115	0.066 ± 0.0071	0.535 ± 0.0125	0.0162 ± 0.0001
GW5074	0.0128	–	–	–
Staurosporine	–	0.00312	0.00344	0.00124

^a Compound **9h** and reference compounds (**GW5074** and **Staurosporine**, positive controls) were tested in a 10-dose singlicate or duplicate IC₅₀ mode with 3-fold serial dilution starting at 20 μM, and the reactions were carried out at 10 μM ATP.

ortho or *meta*-position of 3-trifluoromethylphenyl ring is detrimental for cellular activity. For instance, compound **9d** with fluoro group showed GI₅₀ value of 2.14 ± 0.07 μM, being 31 times less potent than its corresponding analog **9c** with 4-methylimidazole moiety (GI₅₀ = 0.07 ± 0.05 μM). Based on the presented cellular outcomes and considering the poor cellular activity of the previously reported indazole **II** (GI₅₀ values = 6.5 μM), it could be concluded that the currently presented compounds possess distinct improved cellular effects, being more potent than the initially identified indazole **II**. Furthermore, all tested compounds exerted weak cytotoxic effects against the normal cell L132, as indicated by their high GI₅₀ values (>10 μM). Only compound **9h** was an

exception, with GI₅₀ value of 9.27 ± 0.09 μM. However, it still has great selectivity while comparing its GI₅₀ value against K562 cell line (**9h**, GI₅₀ = 0.02 ± 0.02 μM). Based on the aforementioned results, it is obvious that all examined indazoles exhibit differential antiproliferative activity towards leukemia cell K562 rather normal cell L132.

2.3.2. Broader assessment of antileukemic activity by sulforhodamine B (SRB) assay

Intrigued by the promising antiproliferative activity of the target compounds over K562 cell line, the most active members **9h** and **10c** were selected for further broad screening against a panel of six

Table 3

In vitro antiproliferative activity (GI_{50} , μM) of the target compounds against K562 human leukemia cell line and L132 normal cell.

Compound No.	GI_{50} (μM)	
	K562 ^a	L132 ^a
9a	1.54 ± 0.47	>100
9b	>10	ND ^b
9c	0.07 ± 0.05	10.89 ± 1.79
9d	2.14 ± 0.07	>100
9e	2.21 ± 0.43	>100
9f	2.35 ± 1.01	>100
9g	1.48 ± 0.30	>10
9h	0.02 ± 0.02	9.27 ± 0.09
10a	3.47 ± 0.63	15.34 ± 0.32
10b	0.52 ± 0.16	>100
10c	0.15 ± 0.04	12.91 ± 0.71
10d	0.30 ± 0.05	>100
10e	0.83 ± 0.35	16.67 ± 0.46
10f	3.81 ± 0.95	>100
10g	0.57 ± 0.19	>100
Imatinib	0.80 ± 0.14	>10
Indazole II^b	6.50	–

^a GI_{50} were obtained after incubation for 72 h, and the presented values are the average of at least two independent measurements.

^b Reported data [31].

human leukemia cell lines at National Cancer Institute (NCI, Developmental Therapeutics Program, Bethesda, MD, USA). Applying the highly sensitive sulforhodamine B (SRB) assay [37], both compounds were tested initially at a single dose concentration of 10 μM , and GI_{50} values were further assessed by advancing **9h** and **10c** to five dose testing mode (Fig. 6), and compared with the FDA approved drug imatinib (Table 4).

Inspection of the single dose screening data revealed the pronounced antiproliferative activity of both compounds **9h** and **10c** (Growth inhibition (GI) > 80%), being superior to imatinib over all tested leukemia cells. For example, compound **9h** exerted strong cytostatic activity against K562 and HL60(TB) cell lines with GI values of 99.01% and 97.96%, respectively. Moreover, it evinced sound lethal effect (GI > 100%) over PRMI-8226 cell line. However, the five dose testing results underscored the exceptional selective antiproliferative effects of **9h** and **10c** towards the Bcr-Abl positive

Table 4

The antiproliferative effects (% Growth inhibition (GI) at 10 μM ^a and GI_{50} , μM ^b) of compounds **9h**, **10c** and imatinib over a panel of human leukemia cell lines.

Cell line	9h		10c		Imatinib	
	% GI	GI_{50}	% GI	GI_{50}	% GI	GI_{50}
CCRF-CEM	89.49	1.36	85.04	4.88	6.60	16.98
K562	99.01	< 0.01	96.83	< 0.01	NT	0.02
HL60(TB)	97.96	1.40	87.50	3.22	NI	13.49
MOLT-4	92.33	1.31	79.28	3.84	18.00	5.13
RPMI-8226	L	1.98	86.19	4.54	12.60	6.05
SR	87.42	2.40	71.72	5.06	14.60	7.14

^a L: lethal effect (% GI > 100), NT; not tested, NI; no inhibition.

^b Bold figures refer to GI_{50} less than 10 nM.

leukemia cell K562 with GI_{50} values of less than 10 nM, being more potent than imatinib (GI_{50} = 20 nM). Over other leukemia cells, both **9h** and **10c** displayed GI_{50} values of 1.31–2.40 μM and 3.22–5.06 μM , respectively. In this regard, compounds **9h** and **10c** are approximately 140 and 322 times more potent towards K562 than HL60(TB). Such finding of selective cellular potency of **9h** and **10c** may point out their prospective enzymatic selectivity regarding Bcr-Abl rather the other oncogenic kinases.

2.4. NanoBRET target engagement assay

With the purpose to confirm the ability of the most potent target compound **9h** to inhibit Bcr-Abl kinase inside the cells, we performed this assay against HEK293 cells with NanoLuc®-ABL1 Fusion Vector. The NanoBRET™ Target Engagement (TE) intracellular kinase assay measures compound binding at selected target kinase in intact cells, without perturbation of cellular membrane integrity. The assay is relied on the NanoBRET™ System, an energy transfer technique designed to measure molecular proximity in living cells, where it measures the apparent affinity of the test compound by competitive displacement of the cell-permeable NanoBRET™ tracer reversibly bound to a NanoLuc® fusion protein in cells [38]. Compound **9h** elicited comparable potency to that of the reference compound, dasatinib with EC_{50} as small as 14.6 nM (Fig. 7). This study affirmed that compound **9h** is able to cross the cell membrane and can inhibit Bcr-Abl kinase with strong affinity

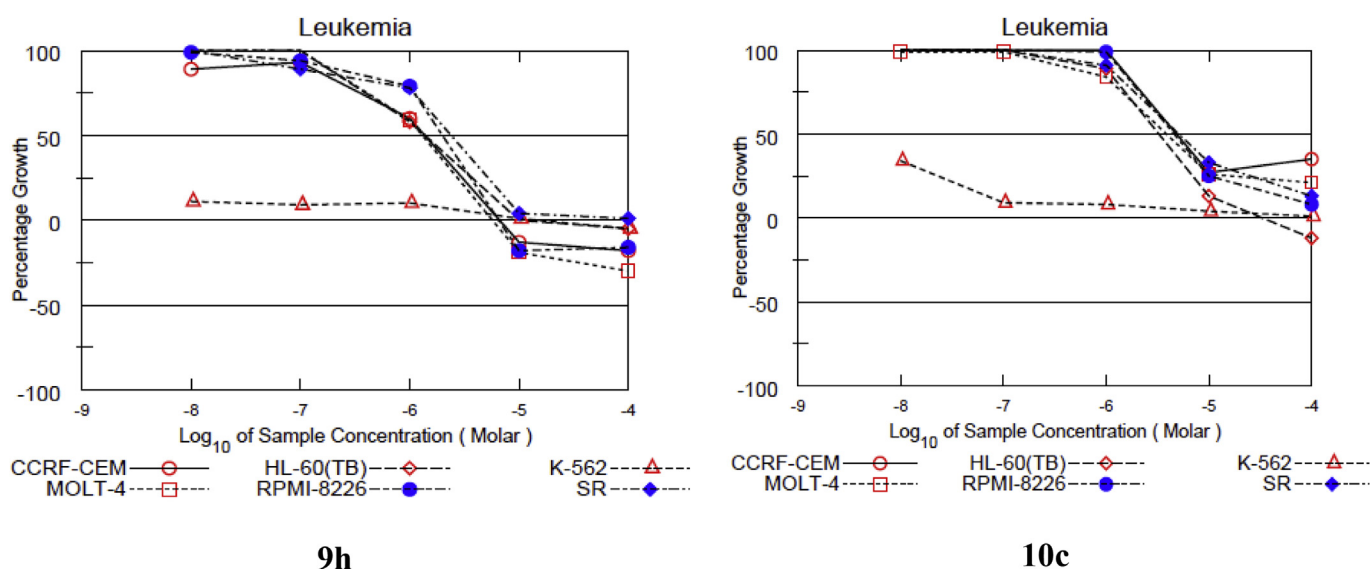


Fig. 6. Dose-response curves of compounds **9h** and **10c** against a panel of six human leukemia cell lines.

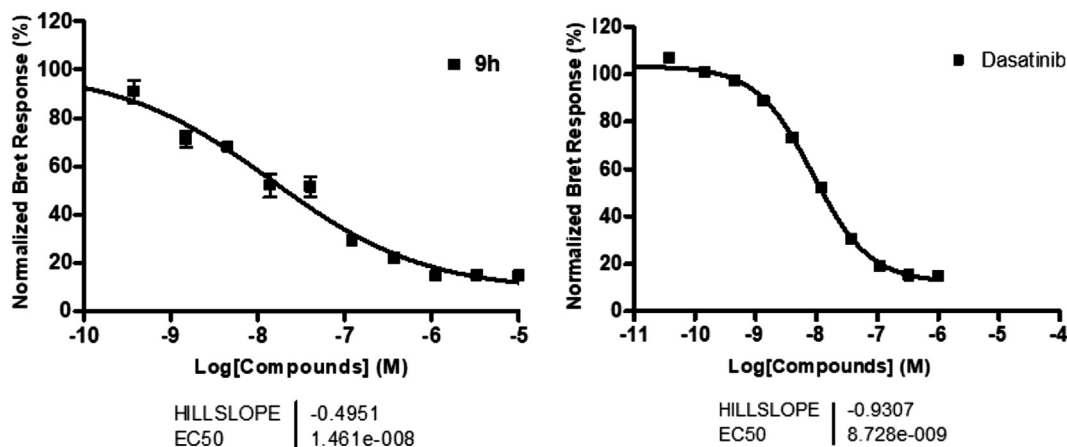


Fig. 7. NanoBRET target engagement assay of compound **9h** and dasatinib using K562 cell line.

inside the cells.

2.5. *In vitro* cellular phosphorylation assay

Furthermore, the effect of compound **9h** on the phosphorylation status of Bcr-Abl kinase was examined using the K562 leukemia cell line harboring Bcr-Abl^{WT}. The K562 cell was treated with five different concentrations (0.003, 0.01, 0.03, 0.1, and 0.3 μ M) of compound **9h**, and its inhibitory activity was compared with that of negative control (DMSO) and dasatinib as a positive control (Fig. 8). As expected, compound **9h** showed a dose-dependent suppression of Bcr-Abl phosphorylation.

2.6. Molecular docking study

To acquire insights about the binding mode of the alkyne-containing indazoles, *in silico* modeling for the most potent member **9h** was conducted using the cocrystal structures of ponatinib-Bcr-Abl^{WT} kinase (PDB 3OXZ) [24] and ponatinib-Bcr-Abl^{T315I} kinase (PDB 3OY3) [24] using Discovery Studio (Fig. 9). As depicted in Fig. 9, compound **9h** adopted a typical type II binding mode (DFG out conformation) to both Bcr-Abl^{WT} and Bcr-Abl^{T315I} kinases, which was illustrated by two canonical hydrogen bonds formed by Glu286, located in the c-Helix, and Asp381, located in the DFG motif, with the amide bond (–NHCO–) of the **9h**. In agreement with our expectations, the NH and nitrogen of 3-aminoindazole moiety of compound **9h** were engaged in multiple hydrogen bonding interactions with the hinge region residues Glu316 and Met318, which are crucial for Bcr-Abl kinase inhibitory activity. Moreover, the 4-morpholino-3-trifluoromethyl phenyl ring was deeply buried into the hydrophobic allosteric pocket, created by DFG shifting. Furthermore, the 3D-binding models revealed that the alkyne linker in compound **9h** made favorable van der Waals interactions with the bulky gatekeeper residue Ile315 avoiding steric clash, which might justify its potent inhibition against Bcr-Abl^{T315I}.

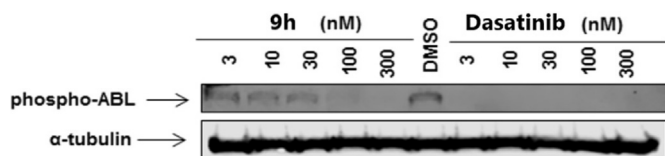


Fig. 8. The effect of compound **9h** on the phosphorylation status of Bcr-Abl kinase in K562 cell line.

2.7. Human ether-a-go-go related gene (hERG) assay

hERG gene encodes the inward rectifying potassium ion channels in the heart, which is involved in cardiac repolarization. Inhibition of the hERG current is known to result in prolongation of the QT interval leading to a serious cardiac disorder called *Torsade de Pointes* [39,40]. Compound **9h** was tested in a 10-dose duplicate assay against hERG, and E-4031 was used as a positive control. The IC₅₀ values are listed in Table 5. The results revealed that compound **9h** is 233 times more selective towards HEK293 cells (nanoBRET assay) than hERG. Also, compound **9h** is 310 folds less potent than E-4031 against hERG. Based on these outcomes, compound **9h** is associated with low risk of QT prolongation.

2.8. *In vivo* pharmacokinetic (PK) profile of 9h

Furthermore, the *in vivo* pharmacokinetic (PK) properties of compound **9h** were evaluated (Table 6). The AUC_{last} values of compound **9h** are 14018.7 ng h/mL and 174.7 ng h/mL following intravenous and oral administration, respectively. **9h** took 0.6 h to reach the maximum concentration (C_{max}) which was 113.0 ng/mL. The low oral exposure of **9h** as indicated by C_{max} along with poor oral bioavailability reveal its unfavorable oral administration. In contrast, intravenous administration of **9h** showed slow clearance and acceptable AUC_{last} and t_{1/2} values to exert its therapeutic effect. Therefore, compound **9h** is better administered as intravenous injection. Design of more orally bioavailable analogues of **9h** and administration of a water-soluble salt of those derivatives are recommended to ameliorate the oral bioavailability.

3. Conclusion

In the current study, we report the design and synthesis of the first series of ethynyl containing 3-aminoindazole as potent Bcr-Abl inhibitors. *In vitro* cell-free and cell-based biological evaluations were performed for all target compounds, and a detailed SAR study has been made. Accordingly, it was evident that the terminal substituted-3-trifluoromethylphenyl ring has a substantial role for achieving favorable Bcr-Abl kinase inhibitory and cellular antileukemic activities. Compounds **9c**, **9h** and **10c** displayed the best potencies outperforming imatinib in both biochemical and cell based assays, with sub-micromolar GI₅₀ values against K562 cell line. Extensive cellular screening of **9h** and **10c** over a panel of six human leukemia cell lines, at NCI, revealed their superior distinct and selective potency towards K562 cell line to imatinib, with GI₅₀

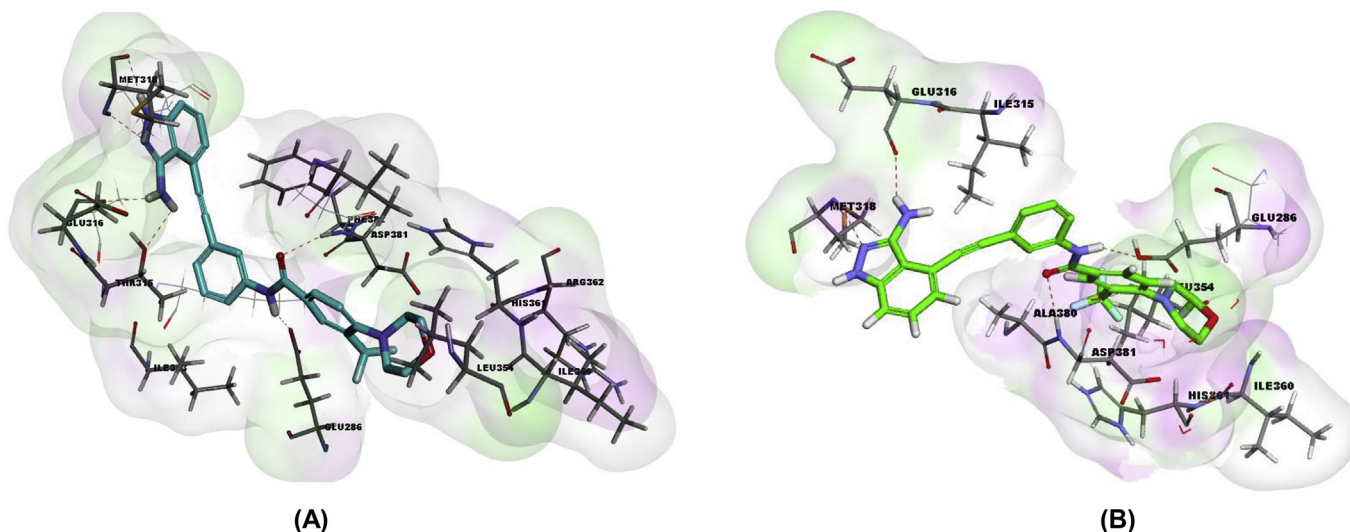


Fig. 9. (A) The putative binding mode of compound **9h** in the kinase domain of Bcr-Abl^{WT}. Carbon atoms of the protein and the ligand are indicated in gray and cyan, respectively. Each dotted line represents a hydrogen bond. (B) The putative binding mode of compound **9h** in the kinase domain of Bcr-Abl^{T315I}. Carbon atoms of the protein and the ligand are indicated in gray and green, respectively. Each red dotted line represents a hydrogen bond. (For interpretation of the references to color in this figure legend, the reader is referred to the Web version of this article.)

Table 5

IC₅₀ of compound **9h** in biochemical hERG assay.

Compound No.	IC ₅₀ (μM) ^a
9h	3.405 ± 0.519
E-4031	0.011 ± 0.002

^a Compounds **9h** and **E-4031** (positive compound) were tested in 10-dose duplicate IC₅₀ mode with a 3-fold serial dilution.

Table 6

In vivo PK parameters of compound **9h** following intravenous (iv) or oral (po) dosing in mice.^a

PK Parameters	IV, 5 mg/kg	PO, 10 mg/kg
T _{max} (h)	– ^b	0.6 ± 0.3
C _{max} (ng/mL)	– ^b	113.0 ± 24.9
T _{1/2} (h)	3.5 ± 1.3	0.7 ± 0.0
AUC _{last} (ng.h/mL)	14018.7 ± 2433.3	174.7 ± 54.1
CL (mL/min/kg)	5.0 ± 1.2	– ^b
MRT _{inf} (h)	4.7 ± 1.3	1.3 ± 0.1
V _{ss} (L/kg)	1.4 ± 0.2	– ^b
F (%)		0.6

^a Values are presented as mean ± SD (n = 3). AUC: area under plasma concentration time curve; C_{max}: peak plasma concentration; T_{max}: time to reach C_{max}; CL: body clearance; MRT_{inf}: mean residence time; V_{ss}: volume of distribution; F: oral bioavailability.

^b Not determined.

less than 10 nM. Out of the 15 target compounds, the morpholine amide derivative **9h** emerged as the most potent member with nanomolar IC₅₀s against Bcr-Abl^{WT}, Bcr-Abl^{T315I} kinases, and their respective K562 cell line overcoming the poor cellular potency of previously reported indazole **II**. The postulated binding mode of **9h** in kinase domain of Bcr-Abl^{WT} and Bcr-Abl^{T315I} disclosed the favorable role of ethynyl linker in avoiding steric repulsion with Ile315 gatekeeper residue. Furthermore, hERG channel inhibition assay for compound **9h** pointed out its low possibility to induce QT prolongation. Taken together, compound **9h** might serve as a promising candidate for further development of potent Bcr-Abl inhibitors for CML therapy.

4. Experimental

4.1. General

All reactions and manipulations were conducted utilizing standard Schlenk techniques. All solvents and reagents were obtained from commercial suppliers and were used without further purification. The reaction progress was monitored on TLC plate (Merck, silica gel 60 F₂₅₄). Flash column chromatography was carried out using silica gel (Merck, 230–400 mesh) and the mobile phase solvents are indicated as a mixed solvent with either given volume-to-volume ratios or as a percentage. ¹H and ¹³C NMR spectra were recorded on a Bruker Avance 400 MHz spectrometer, using appropriate deuterated solvents, as noted. Chemical shifts (δ) are given in parts per million (ppm) upfield from tetramethylsilane (TMS) as internal standard, and br.s, s, d, t, and m are designated as broad singlet, singlet, doublet, triplet and multiplet, respectively. Coupling constants (J) are reported in hertz (Hz). High resolution mass spectra were recorded on Waters Acquity UPLC/Synapt G2 QTOF MS or JMS 700 (Jeol, Japan) mass spectrometer. The purity of all final compounds was >95%, as indicated by ¹H NMR spectra.

4.2. N-(3-Ethynylphenyl)-3-(trifluoromethyl)benzamide (**2a**)

Triethylamine (346 mg, 3.42 mmol) was added slowly to a stirred suspension of 3-ethynylaniline **1** (134 mg, 1.14 mmol) and 3-(trifluoromethyl)benzoyl chloride (286 mg, 1.37 mmol) in dichloromethane (10 mL), and the reaction mixture was stirred at room temperature for 2 h. The solvent was evaporated under reduced pressure and the residue was purified by flash column chromatography on silica gel using (Ethyl acetate-hexane, 1:3 v/v) to afford the title compound as pure yellow solid; 179.4 mg (yield 54.4%); ¹H NMR (400 MHz, CDCl₃) δ 8.55 (s, 1H), 8.09 (s, 1H), 8.01 (d, J = 8.0 Hz, 1H), 7.77–7.74 (m, 2H), 7.66–7.63 (m, 1H), 7.54 (t, J = 7.6 Hz, 1H), 7.29–7.27 (m, 2H), 3.08 (s, 1H); ¹³C NMR (100 MHz, CDCl₃) δ 164.88, 137.52, 135.38, 131.17 (q, J = 33 Hz), 130.48, 129.35, 129.06, 128.70, 128.46 (q, J = 4 Hz), 124.24, 124.17 (q, J = 4 Hz), 123.95 (q, J = 271 Hz), 122.96, 121.34, 82.96, 77.73.

4.3. *N*-(3-Ethynylphenyl)-3,5-bis(trifluoromethyl)benzamide (**2b**)

A stirred suspension of compound **1** (56.6 mg, 0.484 mmol) and 3,5-Bis(trifluoromethyl)benzoyl chloride (161 mg, 0.581 mmol) in pyridine (1 mL) was heated at 90 °C for 1 h. The solvent was evaporated under reduced pressure and the residue was purified by flash column chromatography on silica gel using (Ethyl acetate-hexane, 1:2 v/v) to afford the title compound as pure yellow solid; 91.6 mg (yield 53%); ¹H NMR (400 MHz, Acetone-*d*₆) δ 10.07 (br.s, 1H), 8.64 (s, 2H), 8.29 (s, 1H), 8.04 (s, 1H), 7.85 (d, *J* = 8.2 Hz, 1H), 7.41 (t, *J* = 7.6 Hz, 1H), 7.31 (d, *J* = 7.6 Hz, 1H), 3.68 (s, 1H); ¹³C NMR (100 MHz, Acetone-*d*₆) δ 162.75, 138.88, 137.44, 131.47 (q, *J* = 33 Hz), 129.05, 128.30 (q, *J* = 3 Hz), 127.81, 125.02 (q, *J* = 4 Hz), 123.60, 123.32 (q, *J* = 270 Hz), 122.80, 120.89, 82.97, 78.38; HRMS (ESI-TOF) *m/z* calcd for C₁₇H₁₀F₆NO [M+H]⁺: 358.0667, found: 358.0662.

4.4. General procedure for synthesis of compounds **2c–h**

To a mixture of compound **1** (109 mg, 0.93 mmol) and the appropriate aromatic carboxylic acid (1.21 mmol) in anhydrous DMF (5 mL) under argon atmosphere, DIPEA (3.72 mmol) and HATU (1.21 mmol) were added. The reaction mixture was stirred at rt for 18 h, and then quenched with saturated NaHCO₃ solution (30 mL). The aqueous layer was extracted with ethyl acetate (3 × 20 mL) and the combined organic layers were washed with water and brine, dried over anhydrous Na₂SO₄, filtered, and the solvent was removed under reduced pressure. The resultant residue was purified by flash column chromatography on silica gel using the proper elution system to furnish compounds **2c–h** in pure form.

4.4.1. *N*-(3-Ethynylphenyl)-3-(4-methyl-1H-imidazole-1-yl)-5-(trifluoromethyl)benzamide (**2c**)

Flash column chromatography was carried out using a mixture of hexane and ethyl acetate (1:1 v/v, then switching to 100% ethyl acetate). Yield 41.8%; ¹H NMR (400 MHz, CDCl₃) δ 10.45 (s, 1H), 8.20 (s, 1H), 8.15 (s, 1H), 7.77 (s, 2H), 7.74–7.71 (m, 1H), 7.69 (s, 1H), 7.25–7.24 (m, 2H), 7.03 (s, 1H), 3.04 (s, 1H), 2.09 (s, 3H); ¹³C NMR (100 MHz, CDCl₃) δ 163.88, 140.11, 137.95, 137.66, 137.59, 134.42, 132.79 (q, *J* = 33 Hz), 128.99, 128.70, 124.46, 123.48 (q, *J* = 4 Hz), 123.32, 122.96 (q, *J* = 271 Hz), 122.79, 121.66, 120.23 (q, *J* = 4 Hz), 114.78, 82.97, 77.73, 13.16.

4.4.2. *N*-(3-Ethynylphenyl)-3-fluoro-5-(trifluoromethyl)benzamide (**2d**)

Flash column chromatography was carried out using (Ethyl acetate-hexane, 1:3 v/v). Yield 93.3%; ¹H NMR (400 MHz, CDCl₃) δ 8.06 (s, 1H), 7.91 (s, 1H), 7.80 (d, *J* = 8.4 Hz, 1H), 7.75 (s, 1H), 7.67 (dt, *J* = 6.7 Hz, 2.1 Hz, 1H), 7.54 (d, *J* = 8.0 Hz, 1H), 7.37–7.32 (m, 2H), 3.12 (s, 1H); ¹³C NMR (100 MHz, CDCl₃) δ 163.83, 162.24 (q, *J* = 183 Hz), 137.99, 137.92, 137.14, 129.11 (q, *J* = 22 Hz), 124.02, 123.15, 121.10, 119.58, 119.54, 118.16 (q, *J* = 22 Hz), 116.41, 116.16, 82.79, 77.91.

4.4.3. *N*-(3-Ethynylphenyl)-3-morpholino-5-(trifluoromethyl)benzamide (**2e**)

Flash column chromatography was carried out using (Ethyl acetate-hexane, 1:3 v/v). Yield 84.8%; ¹H NMR (400 MHz, CDCl₃) δ 8.26 (br.s, 1H), 7.77 (s, 1H), 7.71 (dt, *J* = 7.6 Hz, 2.0 Hz, 1H), 7.59 (s, 1H), 7.46 (s, 1H), 7.36–7.29 (m, 2H), 7.24 (s, 1H), 3.88 (t, *J* = 4.8 Hz, 4H), 3.27 (t, *J* = 4.8 Hz, 4H), 3.11 (s, 1H); ¹³C NMR (100 MHz, CDCl₃) δ 165.11, 151.78, 137.70, 136.50, 131.95 (q, *J* = 32 Hz), 129.13, 128.55, 123.87, 123.77 (q, *J* = 271 Hz), 122.97, 121.01, 117.21, 114.47 (q, *J* = 4 Hz), 113.33 (q, *J* = 4 Hz), 83.00, 77.71, 66.52, 48.25; HRMS (ESI-TOF) *m/z* calcd for C₂₀H₁₈F₃N₂O₂ [M+H]⁺: 375.1320, found:

375.1311.

4.4.4. *N*-(3-Ethynylphenyl)-4-methyl-3-(trifluoromethyl)benzamide (**2f**)

Flash column chromatography was carried out using (Ethyl acetate-hexane, 1:3 v/v). Yield 95.2%; ¹H NMR (400 MHz, CDCl₃) δ 8.10 (d, *J* = 1.3 Hz, 1H), 7.99 (br.s, 1H), 7.92 (dd, *J* = 7.9 Hz, 1.8 Hz, 1H), 7.77–7.76 (m, 1H), 7.70 (dt, *J* = 7.6 Hz, 2.0 Hz, 1H), 7.41 (d, *J* = 7.9 Hz, 1H), 7.36–7.31 (m, 2H), 3.10 (s, 1H), 2.57 (s, 3H); ¹³C NMR (100 MHz, CDCl₃) δ 164.49, 141.11, 137.65, 132.52, 132.46, 130.17, 129.15, 128.55, 125.34, 124.55, 124.60, 123.82, 123.02, 120.95, 82.99, 77.69, 19.44; HRMS (ESI-TOF) *m/z* calcd for C₁₇H₁₃F₃NO [M+H]⁺: 304.0949, found: 304.0946.

4.4.5. *N*-(3-Ethynylphenyl)-4-(4-methylpiperazin-1-yl)-3-(trifluoromethyl)benzamide (**2g**)

Flash column chromatography was carried out using (Ethyl acetate-hexane, 1:1 v/v, then switching to 100% ethyl acetate). Yield 64%; ¹H NMR (400 MHz, CDCl₃) δ 8.29 (s, 1H), 8.10 (d, *J* = 1.6 Hz, 1H), 7.97 (dd, *J* = 8.4 Hz, 1.6 Hz, 1H), 7.73 (s, 1H), 7.66 (dt, *J* = 7.0 Hz, 2.0 Hz, 1H), 7.31–7.25 (m, 2H), 3.07 (s, 1H), 3.03 (t, *J* = 4.6 Hz, 4H), 2.59 (br.s, 4H), 2.37 (s, 3H); ¹³C NMR (100 MHz, CDCl₃) δ 164.53, 155.40, 137.77, 131.63, 129.81, 129.05, 128.43, 126.94 (q, *J* = 5 Hz), 125.76 (q, *J* = 29 Hz), 124.0 (q, *J* = 272 Hz), 123.97, 123.23, 122.91, 121.11, 83.04, 77.66, 55.15, 53.01, 46.03.

4.4.6. *N*-(3-Ethynylphenyl)-4-morpholino-3-(trifluoromethyl)benzamide (**2h**)

Flash column chromatography was carried out using (Ethyl acetate-hexane, 1:3 v/v). Yield 97.2%; ¹H NMR (400 MHz, CDCl₃) δ 8.42 (s, 1H), 8.12 (d, *J* = 1.6 Hz, 1H), 8.01 (dd, *J* = 8.4 Hz, 1.6 Hz, 1H), 7.73 (s, 1H), 7.66 (dt, *J* = 6.6 Hz, 2.2 Hz, 1H), 7.32–7.28 (m, 3H), 3.85 (t, *J* = 4.5 Hz, 4H), 3.08 (s, 1H), 2.99 (t, *J* = 4.4 Hz, 4H); ¹³C NMR (100 MHz, CDCl₃) δ 164.53, 154.97, 137.74, 131.86, 130.23, 129.06, 128.49, 126.95 (q, *J* = 6 Hz), 126.17 (q, *J* = 30 Hz), 124.05, 123.62 (q, *J* = 272 Hz), 123.26, 122.91, 121.20, 83.04, 77.71, 67.06, 53.38.

4.5. Methyl-3-iodobenzoate (**4**)

To a stirring solution of 3-iodobenzoic acid **3** (3.00 g, 12.1 mmol) in methanol (75 mL), was added cautiously concentrated H₂SO₄ (3.0 mL), and the resulting solution was refluxed under nitrogen atmosphere for 2.5 h and allowed to cool down to rt. The reaction mixture was then diluted with diethyl ether (75 mL) and washed with H₂O (2 × 75 mL), saturated NaHCO₃ solution (75 mL), and then brine (75 mL). The organic layer was dried over anhydrous Na₂SO₄, filtered, and the solvent was removed under reduced pressure to afford compound **4** as a white solid (3.17 g, 99%); ¹H NMR (400 MHz, CDCl₃) δ 8.35 (t, *J* = 1.6 Hz, 1H), 7.98 (m, 1H), 7.86 (m, 1H), 7.16 (t, *J* = 7.8 Hz, 1H), 3.89 (s, 3H).

4.6. Methyl 3-((trimethylsilyl)ethynyl)benzoate (**5**)

A stirring mixture of compound **4** (3.22 g, 12.29 mmol), trimethylsilylacetylene (1.811 g, 18.4 mmol), PdCl₂(PPh₃)₂ (86 mg, 0.123 mmol) and Et₃N (20 mL) was dissolved in anhydrous THF (40 mL). The reaction mixture was degassed and stirred under argon atmosphere for 15 min before the addition of CuI (36 mg, 0.184 mmol). The reaction was stirred at rt for 18 h, and then was diluted with diethyl ether (75 mL), washed with 0.1 M HCl solution (2 × 100 mL), H₂O (75 mL) and brine (75 mL). The organic layer was dried over anhydrous Na₂SO₄, filtered, and the solvent was removed under reduced pressure to afford **5** as an orange oil (3.41 g, 96%); ¹H NMR (400 MHz, CDCl₃) δ 8.16 (t, *J* = 1.5 Hz, 1H), 7.98 (dt, *J* = 7.8, 1.2 Hz, 1H), 7.65 (dt, *J* = 7.7, 1.2 Hz, 1H), 7.39 (t, *J* = 7.8 Hz, 1H),

3.93 (s, 3H), 0.28 (s, 9H); ^{13}C NMR (100 MHz, CDCl_3) δ 166.33, 136.0, 133.10, 130.30, 129.42, 128.36, 123.59, 103.86, 95.35, 52.23, 0.13.

4.7. 3-Ethynylbenzoic acid (**6**)

Sodium hydroxide (2 N aqueous solution, 15 mL, 28 mmol) was added to a cold solution of compound **5** (3.23 g, 13.9 mmol) in MeOH (75 mL) at 0 °C, and the solution was stirred for 1 h at rt. The reaction mixture was concentrated under reduced pressure, acidified with HCl (2 N aqueous solution), diluted with EtOAc and then washed with water and saturated brine. The organic layer was dried over anhydrous Na_2SO_4 , filtered, and the solvent was removed under reduced pressure to afford **6** as a light brown solid (1.712 g, 84.3%); ^1H NMR (400 MHz, $\text{DMSO}-d_6$) δ 13.0 (br.s, 1H), 7.98–7.96 (m, 2H), 7.73 (dt, $J = 7.8$ Hz, 1.4 Hz, 1H), 7.54 (t, $J = 7.8$ Hz, 1H), 4.30 (s, 1H); ^{13}C NMR (100 MHz, CDCl_3) δ 166.91, 136.23, 132.69, 131.79, 130.13, 129.66, 122.57, 82.93, 82.12.

4.8. General procedure for synthesis of compounds **7a–g**

To a mixture of 3-ethynylbenzoic acid **6** (100 mg, 0.684 mmol) and the appropriate aniline derivative (0.684 mmol) in anhydrous DMF (1 mL) under argon atmosphere, DIPEA (0.45 mL, 2.737 mmol) and HATU (520.3 mg, 1.368 mmol) were added. The reaction mixture was stirred at 60 °C for 4 h, and then quenched with saturated NaHCO_3 solution (10 mL). The aqueous layer was extracted with ethyl acetate (3×10 mL) and the combined organic layers were washed with water and brine, dried over anhydrous Na_2SO_4 , filtered, and the solvent was removed under reduced pressure. The resultant oily residue was purified by flash column chromatography on silica gel using the proper elution system to afford compounds **7a–g** in pure form.

4.8.1. 3-Ethynyl-*N*-(3-(trifluoromethyl)phenyl)benzamide (**7a**)

Flash column chromatography was carried out using (Ethyl acetate-hexane, 1:3 v/v). Yield 73.6%; ^1H NMR (400 MHz, CDCl_3) δ 8.34 (s, 1H), 7.94 (m, 2H), 7.87–7.83 (m, 2H), 7.64 (d, $J = 7.6$ Hz, 1H), 7.48–7.39 (m, 3H), 3.15 (s, 1H); ^{13}C NMR (100 MHz, CDCl_3) δ 165.34, 138.24, 135.47, 134.64, 131.60, 131.28, 130.57, 129.62, 128.96, 127.54, 123.52, 122.96, 121.33 (q, $J = 3.9$ Hz), 117.18 (q, $J = 4.1$ Hz), 82.36, 78.67.

4.8.2. *N*-(3,5-Bis(trifluoromethyl)phenyl)-3-ethynylbenzamide (**7b**)

Flash column chromatography was carried out using (Ethyl acetate-hexane, 1:4 v/v). Yield 23.8%; ^1H NMR (400 MHz, CDCl_3) δ 8.35 (br.s, 1H), 8.19 (s, 2H), 7.97 (s, 1H), 7.88 (d, $J = 7.6$ Hz, 1H), 7.71–7.67 (m, 2H), 7.48 (t, $J = 7.6$ Hz, 1H), 3.18 (s, 1H); ^{13}C NMR (100 MHz, CDCl_3) δ 165.29, 139.11, 135.89, 134.02, 132.49 (q, $J = 33$ Hz), 130.47, 129.16, 127.54, 123.19, 123.00 (q, $J = 271$ Hz), 119.98, 118.05, 82.13, 78.91.

4.8.3. 3-Ethynyl-*N*-(3-(4-methyl-1*H*-imidazole-1-yl)-5-(trifluoromethyl)phenyl)benzamide (**7c**)

Flash column chromatography was carried out using (Ethyl acetate-hexane, 1:2 v/v, then switching to 100% ethyl acetate). Yield 52.3%; ^1H NMR (400 MHz, CDCl_3) δ 9.62 (s, 1H), 8.16 (t, $J = 1.8$ Hz, 1H), 8.00 (t, $J = 1.5$ Hz, 1H), 7.93 (s, 1H), 7.89 (dt, $J = 8.0$ Hz, 1.5 Hz, 1H), 7.86 (d, $J = 1.1$ Hz, 1H), 7.60 (dt, $J = 7.7$ Hz, 1.2 Hz, 1H), 7.39 (t, $J = 7.8$ Hz, 1H), 7.32 (s, 1H), 7.06 (s, 1H), 3.10 (s, 1H), 2.22 (s, 3H); ^{13}C NMR (100 MHz, CDCl_3) δ 165.76, 140.73, 138.33, 138.03, 135.60, 134.41, 134.25, 132.87 (q, $J = 33$ Hz), 131.00, 128.89, 127.85, 123.18 (q, $J = 271$ Hz), 122.84, 120.54, 115.57 (q, $J = 3$ Hz), 114.80, 112.88 (q, $J = 4$ Hz), 82.32, 78.67, 13.21.

4.8.4. 3-Ethynyl-*N*-(3-((4-methylpiperazin-1-yl)methyl)-5-(trifluoromethyl)phenyl)benzamide (**7d**)

Flash column chromatography was carried out using (5% methanol in ethyl acetate). Yield 67.7%; ^1H NMR (400 MHz, CDCl_3) δ 8.04 (br.s, 1H), 7.97 (t, $J = 1.5$ Hz, 1H), 7.93 (s, 1H), 7.87 (dt, $J = 7.9$ Hz, 1.5 Hz, 1H), 7.76 (s, 1H), 7.66 (dt, $J = 7.7$ Hz, 1.3 Hz, 1H), 7.46 (t, $J = 7.8$ Hz, 1H), 7.37 (s, 1H), 3.55 (s, 2H), 3.16 (s, 1H), 2.54 (br.s, 8H), 2.36 (s, 3H); ^{13}C NMR (100 MHz, CDCl_3) δ 164.92, 140.66, 138.34, 135.54, 134.69, 131.52 (q, $J = 34$ Hz), 130.50, 129.08, 127.54, 125.39, 123.55, 123.06, 121.67 (q, $J = 4$ Hz), 115.93 (q, $J = 17$ Hz), 82.36, 78.72, 62.11, 54.95, 52.60, 45.70.

4.8.5. 3-Ethynyl-*N*-(3-(morpholinomethyl)-5-(trifluoromethyl)phenyl)benzamide (**7e**)

Flash column chromatography was carried out using (Ethyl acetate-hexane, 1:1 v/v, then switching to 100% ethyl acetate). Yield 44.7%; ^1H NMR (400 MHz, CDCl_3) δ 8.10 (s, 1H), 7.97 (s, 1H), 7.93 (s, 1H), 7.88–7.86 (m, 2H), 7.67 (d, $J = 7.5$ Hz, 1H), 7.46 (t, $J = 7.7$ Hz, 1H), 7.39 (s, 1H), 3.75 (t, $J = 4.2$ Hz, 4H), 3.59 (s, 2H), 3.16 (s, 1H), 2.51 (t, $J = 4.3$ Hz, 4H); ^{13}C NMR (100 MHz, CDCl_3) δ 164.94, 138.50, 135.56, 134.67, 131.61 (q, $J = 33$ Hz), 130.49, 129.08, 127.57, 125.14, 124.21, 123.76, 123.06, 121.82 (q, $J = 4$ Hz), 116.19 (q, $J = 3$ Hz), 82.36, 78.73, 66.67, 62.58, 53.47.

4.8.6. *N*-(4-Chloro-3-(trifluoromethyl)phenyl)-3-ethynylbenzamide (**7f**)

Flash column chromatography was carried out using (Ethyl acetate-hexane, 1:3 v/v). Yield 38.3%; ^1H NMR (400 MHz, CDCl_3) δ 8.63 (br.s, 1H), 7.96 (d, $J = 2.4$ Hz, 1H), 7.91 (s, 1H), 7.85–7.80 (m, 2H), 7.63 (d, $J = 7.6$ Hz, 1H), 7.44–7.37 (m, 2H), 3.15 (s, 1H); ^{13}C NMR (100 MHz, CDCl_3) δ 165.58, 136.55, 135.60, 134.27, 131.97, 130.61, 128.91 (q, $J = 5$ Hz), 128.58, 127.53, 127.43, 124.54, 122.48 (q, $J = 272$ Hz), 122.96, 119.56 (q, $J = 5$ Hz), 82.26, 78.75.

4.8.7. 3-Ethynyl-*N*-(4-(morpholinomethyl)-3-(trifluoromethyl)phenyl)benzamide (**7g**)

Flash column chromatography was carried out using (Ethyl acetate-hexane, 1:2 then 1:1 v/v, and finally switching to 100% ethyl acetate). Yield 43.5%; ^1H NMR (400 MHz, CDCl_3) δ 8.24 (s, 1H), 7.98 (s, 1H), 7.91–7.87 (m, 3H), 7.79 (d, $J = 8.4$ Hz, 1H), 7.68 (d, $J = 7.6$ Hz, 1H), 7.46 (t, $J = 8.0$ Hz, 1H), 3.75 (t, $J = 4.6$ Hz, 4H), 3.65 (s, 2H), 3.18 (s, 1H), 2.50 (t, $J = 4.2$ Hz, 4H); ^{13}C NMR (100 MHz, CDCl_3) δ 165.11, 136.60, 135.45, 134.71, 133.40, 131.46, 130.51, 129.38 (q, $J = 31$ Hz), 128.98, 128.09, 127.59, 123.52 (q, $J = 271$ Hz), 122.64, 117.75 (q, $J = 6$ Hz), 82.40, 78.67, 67.07, 58.25, 53.59; HRMS (ESI-TOF) m/z calcd for $\text{C}_{21}\text{H}_{20}\text{F}_3\text{N}_2\text{O}_2$ [M+H] $^+$: 389.1477, found: 389.1473.

4.9. 4-Iodo-1*H*-indazol-3-amine (**8**) [26]

A mixture of 2-fluoro-6-iodobenzonitrile (3.0 g, 12.145 mmol) and hydrazine monohydrate (8 mL) in *n*-butanol (40 mL) was stirred and heated at 110 °C for 2 h. The reaction mixture was cooled to room temperature and quenched with a mixture of ethyl acetate and water. The aqueous layer was extracted with ethyl acetate (3×50 mL) and the combined organic layers were washed with water and brine, dried over anhydrous Na_2SO_4 , filtered, and the solvent was removed under reduced pressure to afford the title compound as pure brown solid; 3.084 g (yield 98%); ^1H NMR (400 MHz, $\text{DMSO}-d_6$) δ 11.80 (s, 1H), 7.35 (d, $J = 7.2$ Hz, 1H), 7.30 (d, $J = 8.4$ Hz, 1H), 6.94 (t, $J = 7.6$ Hz, 1H), 5.06 (s, 2H); ^{13}C NMR (100 MHz, $\text{DMSO}-d_6$) δ 148.98, 141.90, 128.74, 128.10, 115.02, 110.52, 86.35.

4.10. General procedure for synthesis of compounds **9a–h** and **10a–g**

To a stirred solution of compound **8** (75 mg, 0.29 mmol) and the appropriate acetylene derivative **2a–h** or **7a–g** (0.29 mmol) in DMF/Et₃N, 1:1 (4 mL) was added PdCl₂(PPh₃)₂ (4.2 mg, 0.006 mmol) and CuI (2.3 mg, 0.012 mmol). The solution was purged with argon for 15 min, sealed, and heated at 85–90 °C for 18 h. The solvents were evaporated under reduced pressure and to the residue was added H₂O and ethyl acetate (10 mL each). The organic layer was separated, and the aqueous layer was repeatedly extracted with ethyl acetate (3 × 10 mL). The combined organic layers were washed with brine solution, dried over anhydrous Na₂SO₄, and filtered. The solvent was evaporated under reduced pressure, and the resulting residue was purified by flash column chromatography on silica gel using the proper elution system to yield compounds **9a–h** and **10a–g** in pure form.

4.10.1. *N*-(3-((3-Amino-1*H*-indazol-4-yl)ethynyl)phenyl)-3-(trifluoromethyl)benzamide (**9a**)

Flash column chromatography was carried out using (Ethyl acetate-hexane, 1:1 then switching to 2:1, v/v). Yield 56%; ¹H NMR (400 MHz, Acetone-*d*₆) δ 11.14 (br. s, 1H), 10.00 (s, 1H), 8.37–8.34 (m, 2H), 8.18 (s, 1H), 7.97–7.94 (m, 2H), 7.81 (t, *J* = 7.7 Hz, 1H), 7.50–7.41 (m, 3H), 7.32 (t, *J* = 8.2 Hz, 1H), 7.22 (d, *J* = 7.0 Hz, 1H), 5.04 (d, *J* = 7.3 Hz, 2H); ¹³C NMR (100 MHz, Acetone-*d*₆) δ 164.29, 139.40 (d, *J* = 9 Hz), 136.07 (d, *J* = 3 Hz), 131.45, 130.26 (q, *J* = 32 Hz), 129.64, 129.20, 128.16 (q, *J* = 4 Hz), 127.17, 127.05, 126.46, 126.34, 124.87, 124.31 (q, *J* = 4 Hz), 124.15 (q, *J* = 270 Hz), 123.17, 123.09, 122.94, 122.84, 120.89, 120.79, 92.91, 87.08; HRMS (FAB+) *m/z* calcd for C₂₃H₁₆F₃N₄O [M+H]⁺: 421.1276, found: 421.1277.

4.10.2. *N*-(3-((3-Amino-1*H*-indazol-4-yl)ethynyl)phenyl)-3,5-bis(trifluoromethyl)benzamide (**9b**)

Flash column chromatography was carried out using (Ethyl acetate-hexane, 1:1 then switching to 2:1, v/v). Yield 62.3%; ¹H NMR (400 MHz, Acetone-*d*₆) δ 10.99 (br. s, 1H), 10.14 (s, 1H), 8.64 (s, 2H), 8.29 (s, 1H), 8.11 (s, 1H), 7.89 (d, *J* = 5.6 Hz, 1H), 7.43–7.33 (m, 4H), 7.20 (d, *J* = 6.0 Hz, 1H), 5.35 (br. s, 2H); ¹³C NMR (100 MHz, Acetone-*d*₆) δ 162.76, 139.04, 137.41, 131.95, 131.62, 131.29, 130.95, 129.24, 128.34, 127.45, 127.36, 125.07, 124.68, 123.65, 123.08, 123.02, 121.98, 120.98, 111.09, 93.25, 86.83; HRMS (FAB+) *m/z* calcd for C₂₄H₁₅F₆N₄O [M+H]⁺: 489.1150, found: 489.1153.

4.10.3. *N*-(3-((3-Amino-1*H*-indazol-4-yl)ethynyl)phenyl)-3-(4-methyl-1*H*-imidazole-1-yl)-5-(trifluoromethyl) benzamide (**9c**)

Flash column chromatography was carried out using (2–5% Methanol in dichloromethane). Yield 33%; ¹H NMR (400 MHz, Acetone-*d*₆) δ 11.10 (br. s, 1H), 10.10 (s, 1H), 8.51 (s, 1H), 8.28 (s, 2H), 8.18 (s, 1H), 8.15 (s, 1H), 7.95 (d, *J* = 8.0 Hz, 1H), 7.57 (s, 1H), 7.52–7.41 (m, 3H), 7.32 (t, *J* = 7.6 Hz, 1H), 7.21 (d, *J* = 6.8 Hz, 1H), 4.98 (br. s, 2H), 2.24 (s, 3H); ¹³C NMR (100 MHz, Acetone-*d*₆) δ 163.39, 149.02, 141.97, 139.95, 139.27, 138.49, 137.96, 134.99, 132.08, 131.76, 129.29, 127.29, 126.36, 124.97, 123.90, 123.24, 122.99, 120.85, 120.00, 115.17, 114.54, 114.12, 112.98, 110.83, 92.75, 87.19; 12.91; HRMS (ESI-TOF) *m/z* calcd for C₂₇H₂₀F₃N₆O [M+H]⁺: 501.1651, found: 501.1650.

4.10.4. *N*-(3-((3-Amino-1*H*-indazol-4-yl)ethynyl)phenyl)-3-fluoro-5-(trifluoromethyl)benzamide (**9d**)

Flash column chromatography was carried out using (Ethyl acetate-hexane, 1:1, v/v then switching to 100% ethyl acetate). Yield 11.3%; ¹H NMR (400 MHz, Acetone-*d*₆) δ 11.02 (br. s, 1H), 9.97 (s, 1H), 8.23 (s, 1H), 8.14–8.11 (m, 2H), 7.92 (d, *J* = 8.0 Hz, 1H), 7.80 (d, *J* = 8.4 Hz, 1H), 7.51–7.40 (m, 3H), 7.31 (t, *J* = 8.0 Hz, 1H), 7.21 (d,

J = 7.2 Hz, 1H), 4.96 (d, *J* = 2.5 Hz, 2H); ¹³C NMR (100 MHz, Acetone-*d*₆) δ 163.75, 162.88, 161.28, 139.19, 129.26, 127.27, 126.37, 123.25, 123.07, 122.94, 122.85, 120.88, 120.78, 120.46, 120.42, 118.80, 118.57, 115.83 (q, *J* = 4 Hz), 115.58 (q, *J* = 4 Hz), 114.56, 110.84, 92.73, 87.17; HRMS (FAB+) *m/z* calcd for C₂₃H₁₅F₄N₄O [M+H]⁺: 439.1182, found: 439.1178.

4.10.5. *N*-(3-((3-Amino-1*H*-indazol-4-yl)ethynyl)phenyl)-3-morpholino-5-(trifluoromethyl)benzamide (**9e**)

Flash column chromatography was carried out using (Ethyl acetate-hexane, 2:1, v/v then switching to 100% ethyl acetate). Yield 58.6%; ¹H NMR (400 MHz, DMSO-*d*₆) δ 11.82 (br. s, 1H), 10.50 (s, 1H), 8.04 (s, 1H), 7.87 (d, *J* = 8.4 Hz, 1H), 7.75 (s, 1H), 7.69 (s, 1H), 7.48 (t, *J* = 7.6 Hz, 1H), 7.41–7.39 (m, 2H), 7.35 (d, *J* = 8.0 Hz, 1H), 7.28 (t, *J* = 8.4 Hz, 1H), 7.16 (d, *J* = 7.2 Hz, 1H), 5.16 (s, 2H), 3.79 (t, *J* = 4.8 Hz, 4H), 3.32–3.31 (m, 4H); ¹³C NMR (100 MHz, DMSO-*d*₆) δ 165.12, 151.95, 141.75, 139.68, 136.90, 130.83, 130.51, 129.79, 127.35, 126.85, 125.95, 123.43, 123.24, 122.78, 121.74, 120.48, 117.70, 114.40, 114.29, 113.98, 111.53, 93.33, 87.59, 66.36, 48.16; HRMS (FAB+) *m/z* calcd for C₂₇H₂₃F₃N₅O₂ [M+H]⁺: 506.1804, found: 506.1806.

4.10.6. *N*-(3-((3-Amino-1*H*-indazol-4-yl)ethynyl)phenyl)-4-methyl-3-(trifluoromethyl)benzamide (**9f**)

Flash column chromatography was carried out using (Ethyl acetate-hexane, 1:1 then switching to 3:1, v/v). Yield 55.2%; ¹H NMR (400 MHz, DMSO-*d*₆) δ 11.83 (s, 1H), 10.55 (s, 1H), 8.28 (s, 1H), 8.19 (d, *J* = 7.6 Hz, 1H), 8.07 (s, 1H), 7.87 (d, *J* = 8.0 Hz, 1H), 7.64 (d, *J* = 7.6 Hz, 1H), 7.48 (t, *J* = 8.0 Hz, 1H), 7.41–7.34 (m, 2H), 7.28 (t, *J* = 8.0 Hz, 1H), 7.16 (d, *J* = 6.8 Hz, 1H), 5.17 (s, 2H), 2.54 (s, 3H); ¹³C NMR (100 MHz, DMSO-*d*₆) δ 164.65, 149.20, 141.77, 140.54, 139.75, 137.00, 133.06, 132.97, 132.06, 129.77, 128.00 (q, *J* = 30 Hz), 127.29, 126.84, 125.45 (q, *J* = 6 Hz), 124.67, 123.38, 123.27 (q, *J* = 6 Hz), 122.74, 121.63, 114.31, 111.52, 93.38, 87.57, 19.27; HRMS (FAB+) *m/z* calcd for C₂₄H₁₈F₃N₄O [M+H]⁺: 435.1432, found: 435.1436.

4.10.7. *N*-(3-((3-Amino-1*H*-indazol-4-yl)ethynyl)phenyl)-4-(4-methylpiperazin-1-yl)-3-(trifluoromethyl)benzamide (**9g**)

Flash column chromatography was carried out using (2–5% Methanol, 1% NH₄OH in dichloromethane). Yield 24.7%; ¹H NMR (400 MHz, Acetone-*d*₆) δ 11.04 (br. s, 1H), 9.85 (s, 1H), 8.32–8.28 (m, 2H), 8.16 (s, 1H), 7.92 (d, *J* = 8.0 Hz, 1H), 7.61 (d, *J* = 8.4 Hz, 1H), 7.47 (t, *J* = 7.9 Hz, 1H), 7.43–7.40 (m, 2H), 7.31 (t, *J* = 8.4 Hz, 1H), 7.20 (d, *J* = 7.0 Hz, 1H), 4.98 (br. s, 2H), 3.06 (t, *J* = 4.7 Hz, 4H), 2.57 (t, *J* = 4.6 Hz, 4H), 2.31 (s, 3H); ¹³C NMR (100 MHz, Acetone-*d*₆) δ 164.07, 155.48, 149.06, 139.64, 132.46, 130.63, 129.16, 127.13, 127.07, 127.03, 126.84, 126.36, 125.51, 125.10, 123.62, 123.13, 123.02, 122.80, 120.77, 114.61, 110.79, 92.91, 87.03, 55.07, 53.01, 45.37; HRMS (ESI-TOF) *m/z* calcd for C₂₈H₂₆F₃N₆O [M+H]⁺: 519.2120, found: 519.2134.

4.10.8. *N*-(3-((3-Amino-1*H*-indazol-4-yl)ethynyl)phenyl)-4-morpholino-3-(trifluoromethyl)benzamide (**9h**)

Flash column chromatography was carried out using (Ethyl acetate-hexane, 2:1, v/v then switching to 100% ethyl acetate). Yield 67.7%; ¹H NMR (400 MHz, Acetone-*d*₆) δ 11.01 (br. s, 1H), 9.84 (s, 1H), 8.34–8.30 (m, 2H), 8.15 (s, 1H), 7.92 (d, *J* = 7.5 Hz, 1H), 7.66 (d, *J* = 8.3 Hz, 1H), 7.49–7.40 (m, 3H), 7.31 (t, *J* = 8.2 Hz, 1H), 7.21 (d, *J* = 7.0 Hz, 1H), 4.97 (br. s, 2H), 3.81 (t, *J* = 4.4 Hz, 4H), 3.04 (t, *J* = 4.3 Hz, 4H); ¹³C NMR (100 MHz, DMSO-*d*₆) δ 164.50, 155.03, 149.05, 141.74, 139.80, 133.47, 130.80, 129.78, 127.50 (q, *J* = 6 Hz), 127.24, 126.83, 124.91, 124.63, 124.33, 123.24, 123.02, 122.73, 121.59, 114.29, 112.72, 111.52, 93.37, 87.56, 66.89, 53.57; HRMS (ESI-TOF) *m/z* calcd for C₂₇H₂₃F₃N₅O₂ [M+H]⁺: 506.1804, found: 506.1807.

4.10.9. 3-((3-Amino-1H-indazol-4-yl)ethynyl)-N-(3-(trifluoromethyl)phenyl)benzamide (**10a**)

Flash column chromatography was carried out using (Ethyl acetate-hexane, 1:1 then 2:1, v/v). Yield 43.7%; ^1H NMR (400 MHz, Acetone- d_6) δ 11.09 (br. s, 1H), 9.98 (s, 1H), 8.36 (s, 1H), 8.28 (s, 1H), 8.14 (d, $J = 8.0$ Hz, 1H), 8.09 (d, $J = 7.6$ Hz, 1H), 7.87 (d, $J = 7.6$ Hz, 1H), 7.66–7.61 (m, 2H), 7.49 (d, $J = 7.6$ Hz, 1H), 7.42 (d, $J = 8.4$ Hz, 1H), 7.33 (t, $J = 8.0$ Hz, 1H), 7.23 (d, $J = 6.8$ Hz, 1H), 5.01 (s, 2H); ^{13}C NMR (100 MHz, Acetone- d_6) δ 164.99, 161.06, 140.08, 135.46, 134.47, 130.61, 130.28, 129.74, 129.07, 128.00, 126.42, 125.76, 123.69, 123.54, 123.46, 123.27, 123.18, 123.05, 120.19 (q, $J = 4$ Hz), 116.56 (q, $J = 4$ Hz), 111.10, 92.14, 87.98; HRMS (FAB+) m/z calcd for $\text{C}_{23}\text{H}_{16}\text{F}_3\text{N}_4\text{O}$ $[\text{M}+\text{H}]^+$: 421.1276, found: 421.1272.

4.10.10. 3-((3-Amino-1H-indazol-4-yl)ethynyl)-N-(3,5-bis(trifluoromethyl)phenyl)benzamide (**10b**)

Flash column chromatography was carried out using (Ethyl acetate-hexane, 1:1 v/v). Yield 12.8%; ^1H NMR (400 MHz, Acetone- d_6) δ 11.12 (br. s, 1H), 10.27 (s, 1H), 8.61 (s, 2H), 8.32 (s, 1H), 8.12 (d, $J = 8.0$ Hz, 1H), 7.88 (d, $J = 7.6$ Hz, 1H), 7.79 (s, 1H), 7.64 (t, $J = 8.0$ Hz, 1H), 7.43 (d, $J = 8.4$ Hz, 1H), 7.32 (t, $J = 8.4$ Hz, 1H), 7.22 (d, $J = 7.2$ Hz, 1H), 5.03 (s, 2H); ^{13}C NMR (100 MHz, Acetone- d_6) δ 165.34, 149.07, 142.02, 141.18, 134.84, 134.81, 131.62 (q, $J = 33$ Hz), 130.33, 129.15, 128.07, 126.41, 124.90, 123.28, 122.20, 120.01 (q, $J = 4$ Hz), 116.65 (q, $J = 4$ Hz), 114.28, 112.96, 111.11, 92.05, 88.13; HRMS (FAB+) m/z calcd for $\text{C}_{24}\text{H}_{15}\text{F}_6\text{N}_4\text{O}$ $[\text{M}+\text{H}]^+$: 489.1150, found: 489.1148.

4.10.11. 3-((3-Amino-1H-indazol-4-yl)ethynyl)-N-(3-(4-methyl-1H-imidazole-1-yl)-5-(trifluoromethyl)phenyl) benzamide (**10c**)

Flash column chromatography was carried out using (5% Methanol in dichloromethane). Yield 11%; ^1H NMR (400 MHz, Acetone- d_6) δ 11.08 (br. s, 1H), 10.16 (s, 1H), 8.42 (s, 1H), 8.30 (s, 1H), 8.25 (s, 1H), 8.12–8.10 (m, 2H), 7.89 (d, $J = 7.6$ Hz, 1H), 7.70–7.65 (m, 2H), 7.44–7.41 (m, 2H), 7.33 (t, $J = 8.4$ Hz, 1H), 7.23 (d, $J = 6.8$ Hz, 1H), 4.98 (s, 2H), 2.24 (s, 3H); ^{13}C NMR (100 MHz, Acetone- d_6) δ 165.18, 165.11, 148.94, 141.51, 141.42, 139.83, 138.68, 135.09 (q, $J = 4$ Hz), 134.70, 131.94 (q, $J = 33$ Hz), 130.27, 129.18, 128.03, 126.35, 123.29, 123.22, 122.49, 114.97, 114.88, 114.33, 114.09, 112.97, 112.04 (q, $J = 4$ Hz), 111.07, 92.01, 88.11, 12.93; HRMS (ESI-TOF) m/z calcd for $\text{C}_{27}\text{H}_{20}\text{F}_3\text{N}_6\text{O}$ $[\text{M}+\text{H}]^+$: 501.1651, found: 501.1650.

4.10.12. 3-((3-Amino-1H-indazol-4-yl)ethynyl)-N-(3-((4-methylpiperazin-1-yl)methyl)-5-(trifluoromethyl)phenyl) benzamide (**10d**)

Flash column chromatography was carried out using (5–10% Methanol, 1% NH_4OH in dichloromethane). Yield 15.6%; ^1H NMR (400 MHz, Acetone- d_6) δ 11.06 (br.s, 1H), 9.94 (s, 1H), 8.09–8.08 (m, 2H), 8.11–8.08 (m, 2H), 7.88 (d, $J = 7.6$ Hz, 1H), 7.65 (t, $J = 8.0$, 1H), 7.44 (s, 1H), 7.42 (s, 1H), 7.33 (t, $J = 8.4$, 1H), 7.23 (d, $J = 6.8$, 1H), 4.96 (d, $J = 10.0$ Hz, 1H), 3.61 (s, 2H), 2.49–2.40 (m, 8H), 2.21 (s, 3H); ^{13}C NMR (100 MHz, Acetone- d_6) δ 164.93, 141.44, 140.05, 139.96, 135.48 (q, $J = 31$ Hz), 134.44, 131.38, 130.48, 130.28, 130.16, 129.24, 129.07, 129.00, 128.00, 126.35, 125.80, 123.68, 123.60, 123.20, 120.38, 115.20 (q, $J = 4$ Hz), 114.31, 111.03, 92.11, 87.98, 61.93, 55.04, 52.98, 45.42; HRMS (ESI-TOF) m/z calcd for $\text{C}_{29}\text{H}_{28}\text{F}_3\text{N}_6\text{O}$ $[\text{M}+\text{H}]^+$: 533.2277, found: 533.2277.

4.10.13. 3-((3-Amino-1H-indazol-4-yl)ethynyl)-N-(3-(morpholinomethyl)-5-(trifluoromethyl)phenyl)benzamide (**10e**)

Flash column chromatography was carried out using (2–5% Methanol in dichloromethane). Yield 41%; ^1H NMR (400 MHz, CDCl_3) δ 8.85 (br.s, 1H), 8.05 (s, 1H), 8.01 (s, 1H), 7.87 (s, 1H), 7.84 (d, $J = 7.8$ Hz, 1H), 7.60 (d, $J = 7.6$ Hz, 1H), 7.37 (t, $J = 7.7$ Hz, 1H), 7.31 (s, 1H), 7.20 (d, $J = 3.7$ Hz, 2H), 7.10 (t, $J = 4.0$ Hz, 1H), 4.96 (br.s, 2H), 3.71 (t, $J = 4.2$ Hz, 4H), 3.56 (s, 2H), 2.51 (s, 4H); ^{13}C NMR (100 MHz,

CDCl_3) δ 165.32, 149.15, 141.94, 138.84, 138.61, 138.44, 134.76, 134.65, 131.43 (q, $J = 32$ Hz), 129.90, 129.04, 127.77, 127.33, 124.17, 123.78 (q, $J = 271$ Hz), 123.14, 121.76 (q, $J = 4$ Hz), 116.53 (q, $J = 3$ Hz), 114.57, 113.20, 110.91, 92.64, 87.93, 66.38, 62.35, 53.26; HRMS (ESI-TOF) m/z calcd for $\text{C}_{28}\text{H}_{25}\text{F}_3\text{N}_5\text{O}_2$ $[\text{M}+\text{H}]^+$: 520.1960, found: 520.1960.

4.10.14. 3-((3-Amino-1H-indazol-4-yl)ethynyl)-N-(4-chloro-3-(trifluoromethyl)phenyl)benzamide (**10f**)

Flash column chromatography was carried out using (Ethyl acetate-hexane, 1:1, v/v then switching to 100% ethyl acetate). Yield 76.2%; ^1H NMR (400 MHz, Acetone- d_6) δ 11.11 (br.s, 1H), 10.11 (s, 1H), 8.46 (s, 1H), 8.28 (s, 1H), 8.21 (d, $J = 8.7$ Hz, 1H), 8.09 (d, $J = 7.8$ Hz, 1H), 7.89 (d, $J = 7.7$ Hz, 1H), 7.71–7.64 (m, 2H), 7.44 (d, $J = 8.3$ Hz, 1H), 7.34 (t, $J = 8.3$ Hz, 1H), 7.24 (d, $J = 7.0$ Hz, 1H), 4.98 (d, $J = 10.0$ Hz, 1H); ^{13}C NMR (100 MHz, Acetone- d_6) δ 165.02, 148.97, 142.01, 138.71, 135.19, 134.61, 131.99, 130.27, 129.12, 128.00, 127.07 (q, $J = 31$ Hz), 126.35, 125.36, 124.67, 124.59, 123.22, 123.04 (q, $J = 271$ Hz), 119.08 (q, $J = 6$ Hz), 114.27, 112.96, 111.06, 92.03, 88.06; HRMS (FAB+) m/z calcd for $\text{C}_{23}\text{H}_{15}\text{ClF}_3\text{N}_4\text{O}$ $[\text{M}+\text{H}]^+$: 455.0886, found: 455.0889.

4.10.15. 3-((3-Amino-1H-indazol-4-yl)ethynyl)-N-(4-(morpholinomethyl)-3-(trifluoromethyl)phenyl)benzamide (**10g**)

Flash column chromatography was carried out using (0–2% Methanol in ethyl acetate). Yield 63.4%; ^1H NMR (400 MHz, $\text{DMSO}-d_6$) δ 11.84 (br.s, 1H), 10.65 (s, 1H), 8.24 (s, 2H), 8.08 (d, $J = 8.4$ Hz, 1H), 8.03 (d, $J = 8.0$ Hz, 1H), 7.87 (d, $J = 7.6$ Hz, 1H), 7.75 (d, $J = 8.4$ Hz, 1H), 7.65 (t, $J = 7.6$ Hz, 1H), 7.37 (d, $J = 8.4$ Hz, 1H), 7.30 (t, $J = 8.4$ Hz, 1H), 7.19 (d, $J = 6.8$ Hz, 1H), 5.16 (s, 2H), 3.60–3.59 (m, 6H), 2.40 (s, 4H); ^{13}C NMR (100 MHz, $\text{DMSO}-d_6$) δ 165.39, 149.06, 141.77, 138.65, 135.50, 134.94, 132.20, 131.88, 130.75, 129.63, 128.78, 128.02 (q, $J = 33$ Hz), 126.81, 126.15, 123.99, 123.38, 122.80, 117.79 (q, $J = 6$ Hz), 114.10, 112.75, 111.70, 92.72, 88.51, 66.70, 58.34, 53.76; HRMS (ESI-TOF) m/z calcd for $\text{C}_{28}\text{H}_{25}\text{F}_3\text{N}_5\text{O}_2$ $[\text{M}+\text{H}]^+$: 520.1960, found: 520.1955.

4.11. In vitro kinase screening

Reaction Biology Corp. Kinase HotSpotSM service was used for biochemical evaluation of compounds **9a–h** and **10a–g** according to the reported assay protocol [34,41].

4.12. In vitro evaluations of antiproliferative activity

4.12.1. Preliminary MTT evaluation of antiproliferative activity

The antiproliferative activity of the target compounds was evaluated against human leukemia K562 cancer cell and L132 normal cell line using the MTT assay following the reported assay procedure [41].

4.12.2. NCI antileukemic screening

The cancer cell screening of compounds **9h** and **10c** over a panel of six human leukemia cell lines was applied using SRB assay at the National Cancer Institute (NCI), Bethesda, Maryland, USA adopting the standard protocol [42].

4.13. NanoBRET target engagement assay

To HEK293 cells transiently transfected with 1 μg ABL1-NanoLuc fusion vector, the test compounds (**9h** and dasatinib as reference) were added. The compounds were tested in a 10-dose testing assay starting with 10 μM (**9h**) or 1 μM (dasatinib) at 3-fold serial dilution. The medium was removed from the dish by aspiration, and trypsin was neutralized using medium containing serum and

centrifuge at 200×g for 5 min to pellet the cells. The cells were prepared with NanoBRET™ Tracer K-4 reagent. The cell suspension was dispensed into white, 384-well NBS plates, and the plate was incubated at 37 °C, 5% CO₂ for 1 h. For optional background correction steps, a separate set of samples without tracer was prepared. After removing the plate from the incubator, it was equilibrated to room temperature for 15 min 3X complete substrate plus inhibitor solution in assay medium (OptiMEMR I reduced serum medium, no phenol red) was prepared just before measuring BRET. 10 μL of 3X complete substrate plus inhibitor solution was added to each well of the 384-well plate, and was incubated for 2–3 min at room temperature. Donor emission wavelength (460 nm) and acceptor emission wavelength (600 nm) were measured in the EnVision plate reader.

4.14. Western blot assay for compound **9h**

This assay was performed at RBC according to the following method. Compound **9h** was dissolved in DMSO at 10 mM stock. 1×10^6 cells/well of K562 cells were seeded in 24-well plates with complete culture media overnight. The cells were treated with test compound **9h** or reference compound dasatinib for 1 h, then cells were collected by centrifugation at 4 °C and resuspended in ice cold PBS. The cells were lysed with 1X Cell Signaling Lysis Buffer plus 1X proteinase/phosphatase inhibitor cocktail and 1 mM PMSF. The lysate samples were centrifuged at 12000 rpm for 10 min at 4 °C. The supernatants were transferred to a new set of Eppendorf tubes. 4X LDS Sample Buffer with DTT was added to the cell lysates. The protein samples were heated at 95 °C for 5 min. Cell lysate samples were subjected to SDS-PAGE with 7% Tris-Acetate gel and transferred onto nitrocellulose membranes by iBlot Dry Blotting System. The membranes were blocked with LI-COR TBS Blocking Buffer for 1 h and then probed with phospho-Abl overnight at 4 °C, washed in TBS Tween, and re-probed with α -tubulin antibody overnight at 4 °C. Anti-rabbit IgG IRDye 680RD and anti-mouse IgG IRDye 800CW secondary antibodies were used to detect the primary antibodies as recommended by the manufacturer. The membranes were scanned with LI-COR Odyssey Fc Imaging System.

4.15. Molecular docking

The docking model of compound **9h** was constructed using the X-ray co-crystal structure of Bcr-Abl^{WT} (PDB: 3OXZ) [24] or Bcr-Abl^{T315I} (PDB: 3OY3) [24], in its DFG-out conformation, with ponatinib. The protein was treated with protein preparation tool applying the default values as implemented in Discovery Studio 2017 R2 client software [43], and conserving water molecules. The binding site was defined based on contacts of ponatinib with Bcr-Abl kinase domain. The ligand was prepared by Ligand Preparation tool implemented in Discovery Studio 2017 R2, and CDOCKER algorithm was used to perform docking of the ligand into the defined binding site. The ligand pose with the best score was selected for analysis of binding mode. The results were visualized and analyzed using tools implemented in Discovery Studio 2017 R2.

4.16. hERG channel assay

The assay is relied on the competition of fluorescently labeled tracer binding to the membrane preparation containing hERG. The used buffer is composed of 25 mM Hepes, pH 7.5, 15 mM KCl, 1 mM MgCl₂, 0.05% PF-127, and 1% DMSO. Solutions of the test compounds in DMSO were added in the test concentration into the membrane mixture (1X Predictor™ hERG Membrane) by using Acoustic Technology. The tracer (1 nM Predictor™ hERG Tracer Red) was added and gently mixed in dark. The fluorescence was

measured at 531 nm after 4 h incubation at room temperature and the membrane potential was calculated. The background was established by the average FP signal in the presence of 30 μM E4031. The IC₅₀ values of the test compounds were estimated using GraphPad Prism software.

4.17. In vivo pharmacokinetic (PK) profile of **9h**

The pharmacokinetic (PK) studies were conducted in accordance with the Animal Ethics Committee (IACUC) of the experimental animal center of Daegu-Gyeongbuk Medical Innovation Foundation (DGMIF) based on the animal protection act. In pharmacokinetic assays, male ICR mice (SPF, ORIENTBIO INC. Korea, 25–30 g, n = 4 (iv) and 4 (po) animals) were treated with a dose of 5 mg/kg and 10 mg/kg of compound **9h** through iv and po, respectively. The formulation of vehicle was 10% DMSO, 10% cremophor EL and 80% saline in both iv and po. The mice were followed 7 days acclimation to the vivarium. Blood samples (each 0.3 mL) were collected at 0, 0.08, 0.25, 0.5, 1, 2, 4, 6 and 8 h (iv), and 0, 0.25, 0.5, 1, 2, 4, 6 and 8 h (po) into microtubes (QSP, 1.5 mL). Following centrifugation at 4 °C, the plasma was stored at -70 ± 10 °C for LC-MS analysis. Compound levels in plasma were quantitatively analyzed by LC-MS/MS (Triple Quad 5500, Applied Biosystems, USA) following protein precipitation with acetonitrile including an internal standard. PK parameters were calculated from the normalized LC-MS/MS peak areas using a non-compartmental analysis model with WinNonlin 6.4 version (Pharsight, USA).

Declaration of competing interest

The authors declare that they have no known competing financial interests or personal relationships that could have appeared to influence the work reported in this paper.

Acknowledgments

This research was supported by Bio & Medical Technology Development Program (NRF-2019M3E5D4066905) and Korea Research Fellowship Program (NRF-2019H1D3A1A01070882) of the National Research Foundation funded by the Korean government (MSIT), and by the Korea Institute of Science and Technology Institutional Programs (Grant No. 2E30180 and 2Z05800). We would like to express our genuine gratitude and appreciation to the National Cancer Institute (NCI, Bethesda, Maryland, USA) for performing the *in vitro* anticancer evaluation of compounds **9h** and **10c**.

Appendix A. Supplementary data

Supplementary data to this article can be found online at <https://doi.org/10.1016/j.ejmech.2020.112710>.

References

- [1] C.L. Sawyers, Chronic myeloid leukemia, *N. Engl. J. Med.* 340 (1999) 1330–1340.
- [2] A. Rana, S.H. Shah, N. Rehman, S. Ali, S. Bhatti, A.A. Farooqi, Chronic myeloid leukemia: attributes of break point cluster region-abelson (BCR-ABL), *J. Canc. Res. Exp. Oncol.* 3 (2011) 62–66.
- [3] E.K. Greuber, P. Smith-Pearson, J. Wang, A.M. Pendergast, Role of ABL family kinases in cancer: from leukaemia to solid tumours, *Nat. Rev. Canc.* 13 (2013) 559–571.
- [4] R. Ren, Mechanisms of BCR-ABL in the pathogenesis of chronic myelogenous leukaemia, *Nat. Rev. Canc.* 5 (2005) 172–183.
- [5] R. Capdeville, E. Buchdunger, J. Zimmermann, A. Matter, Glivec (STI571, imatinib), a rationally developed, targeted anticancer drug, *Nat. Rev. Drug Discov.* 1 (2002) 493–502.
- [6] H. Kantarjian, C. Sawyers, A. Hochhaus, F. Guilhot, C. Schiffer, C. Gambacorti-

- Passerini, D. Niederwieser, D. Resta, R. Capdeville, U. Zoellner, et al., Hematologic and cytogenetic responses to imatinib mesylate in chronic myelogenous leukemia, *N. Engl. J. Med.* 346 (2002) 645–652.
- [7] B. Nagar, W.G. Bornmann, P. Pellicena, T. Schindler, D.R. Veach, W.T. Miller, B. Clarkson, J. Kuriyan, Crystal structures of the kinase domain of c-Abl in complex with the small molecule inhibitors PD173955 and imatinib (STI-571), *Canc. Res.* 62 (2002) 4236–4243.
- [8] T. Schindler, W. Bornmann, P. Pellicena, W.T. Miller, B. Clarkson, J. Kuriyan, Structural mechanism for STI-571 inhibition of abelson tyrosine kinase, *Science* 289 (2000) 1938–1942.
- [9] M.E. Gorre, M. Mohammed, K. Ellwood, N. Hsu, R. Paquette, P.N. Rao, C.L. Sawyers, Clinical resistance to STI-571 cancer therapy caused by BCR-ABL gene mutation or amplification, *Science* 293 (2001) 876–880.
- [10] T. O'Hare, C.A. Eide, M.W. Deininger, Bcr-Abl kinase domain mutations, drug resistance, and the road to a cure for chronic myeloid leukemia, *Blood* 110 (2007) 2242–2249.
- [11] T. O'Hare, D.K. Walters, E.P. Stoffregen, T. Jia, P.W. Manley, J. Mestan, S.W. Cowan-Jacob, F.Y. Lee, M.C. Heinrich, M.W. Deininger, B.J. Druker, In vitro activity of Bcr-Abl inhibitors AMN107 and BMS-354825 against clinically relevant imatinib-resistant Abl kinase domain mutants, *Canc. Res.* 65 (2005) 4500–4505.
- [12] E. Jabbour, J. Cortes, H. Kantarjian, Treatment selection after imatinib resistance in chronic myeloid leukemia, *Targeted Oncol.* 4 (2009) 3–10.
- [13] A. Quintás-Cardama, J. Cortes, Therapeutic options against BCR-ABL1 T315I-positive chronic myelogenous leukemia, *Clin. Canc. Res.* 14 (2008) 4392–4399.
- [14] E. Weisberg, P.W. Manley, W. Breitenstein, J. Brügger, S.W. Cowan-Jacob, A. Ray, B. Huntly, D. Fabbro, G. Fendrich, E. Hall-Meyers, et al., Characterization of AMN107, a selective inhibitor of native and mutant Bcr-Abl, *Canc. Cell* 7 (2005) 129–141.
- [15] F. Santos, H. Kantarjian, J. Cortes, A. Quintás-Cardama, Bafetinib, a dual Bcr-Abl/Lyn tyrosine kinase inhibitor for the potential treatment of leukemia, *Curr. Opin. Invest. Drugs* 11 (2010) 1450–1465.
- [16] L.J. Lombardo, F.Y. Lee, P. Chen, D. Norris, J.C. Barrish, K. Behnia, S. Castaneda, L.A. Cornelius, J. Das, A.M. Doweyko, et al., Discovery of N-(2-chloro-6-methylphenyl)-2-(6-(4-(2-hydroxyethyl)-piperazin-1-yl)-2-methylpyrimidin-4-ylamino) thiazole-5-carboxamide (BMS-354825), a dual Src/Abl kinase inhibitor with potent antitumor activity in preclinical assays, *J. Med. Chem.* 47 (2004) 6658–6661.
- [17] D.H. Boschelli, F. Ye, Y.D. Wang, M. Dutia, S.L. Johnson, B. Wu, K. Miller, D.W. Powell, D. Yaczko, M. Young, et al., Optimization of 4-phenylamino-3-quinolinecarboxitriles as potent inhibitors of Src kinase activity, *J. Med. Chem.* 44 (2001) 3965–3977.
- [18] H.G. Choi, P. Ren, F. Adrian, F. Sun, H.S. Lee, X. Wang, Q. Ding, G. Zhang, Y. Xie, J. Zhang, et al., A type-II kinase inhibitor capable of inhibiting the T315I "gatekeeper" mutant of Bcr-Abl, *J. Med. Chem.* 53 (2010) 5439–5448.
- [19] X. Deng, B. Okram, Q. Ding, J. Zhang, Y. Choi, F.J. Adrián, A. Wojciechowski, G. Zhang, J. Che, B. Bursulaya, et al., Expanding the diversity of allosteric bcr-abl inhibitors, *J. Med. Chem.* 53 (2010) 6934–6946.
- [20] W.-S. Huang, C.A. Metcalf, R. Sundaramoorthi, Y. Wang, D. Zou, R.M. Thomas, X. Zhu, L. Cai, D. Wen, S. Liu, et al., Discovery of 3-[2-(imidazo [1, 2-b] pyridazin-3-yl) ethynyl]-4-methyl-N-{4-[(4-methylpiperazin-1-yl) methyl]-3-(trifluoromethyl) phenyl} benzamide (AP24534), a potent, orally active pan-inhibitor of breakpoint cluster region-abelson (BCR-ABL) kinase including the T315I gatekeeper mutant, *J. Med. Chem.* 53 (2010) 4701–4719.
- [21] Y. Li, M. Shen, Z. Zhang, J. Luo, X. Pan, X. Lu, H. Long, D. Wen, F. Zhang, F. Leng, et al., Design, synthesis, and biological evaluation of 3-(1 H-1, 2, 3-triazol-1-yl) benzamide derivatives as potent pan Bcr-Abl inhibitors including the threonine315→ isoleucine315 mutant, *J. Med. Chem.* 55 (2012) 10033–10046.
- [22] X. Ren, X. Pan, Z. Zhang, D. Wang, X. Lu, Y. Li, D. Wen, H. Long, J. Luo, Y. Feng, et al., Identification of GZD824 as an orally bioavailable inhibitor that targets phosphorylated and nonphosphorylated breakpoint cluster region–Abelson (Bcr-Abl) kinase and overcomes clinically acquired mutation-induced resistance against imatinib, *J. Med. Chem.* 56 (2013) 879–894.
- [23] T. O'Hare, W.C. Shakespeare, X. Zhu, C.A. Eide, V.M. Rivera, F. Wang, L.T. Adrian, T. Zhou, W.-S. Huang, Q. Xu, et al., AP24534, a pan-BCR-ABL inhibitor for chronic myeloid leukemia, potently inhibits the T315I mutant and overcomes mutation-based resistance, *Canc. Cell* 16 (2009) 401–412.
- [24] T. Zhou, L. Commodore, W.S. Huang, Y. Wang, M. Thomas, J. Keats, Q. Xu, V.M. Rivera, W.C. Shakespeare, T. Clackson, et al., Structural mechanism of the pan-BCR-ABL inhibitor ponatinib (AP24534): lessons for overcoming kinase inhibitor resistance, *Chem. Biol. Drug Des.* 77 (2011) 1–11.
- [25] X. Liu, A. Kung, B. Malinoski, G.S. Prakash, C. Zhang, Development of alkyne-containing pyrazolopyrimidines to overcome drug resistance of Bcr-Abl kinase, *J. Med. Chem.* 58 (2015) 9228–9237.
- [26] Y. Dai, K. Hartandi, Z. Ji, A.A. Ahmed, D.H. Albert, J.L. Bauch, J.J. Bouska, P.F. Bousquet, G.A. Cunha, K.B. Glaser, et al., Discovery of N-(4-(3-Amino-1 H-indazol-4-yl) phenyl)-N-(2-fluoro-5-methylphenyl) urea (ABT-869), a 3-aminoindazole-based orally active multitargeted receptor tyrosine kinase inhibitor, *J. Med. Chem.* 50 (2007) 1584–1597.
- [27] Z. Ji, Y. Dai, C. Abad-Zapatero, D.H. Albert, J.J. Bouska, K.B. Glaser, P.A. Marcotte, N.B. Soni, T.J. Magoc, K.D. Stewart, et al., Exploration of diverse hinge-binding scaffolds for selective Aurora kinase inhibitors, *Bioorg. Med. Chem. Lett.* 22 (2012) 4528–4531.
- [28] Y. Lv, M. Li, T. Liu, L. Tong, T. Peng, L. Wei, J. Ding, H. Xie, W. Duan, Discovery of a new series of naphthamides as potent VEGFR-2 kinase inhibitors, *ACS Med. Chem. Lett.* 5 (2014) 592–597.
- [29] Y. Sun, Y. Shan, C. Li, R. Si, X. Pan, B. Wang, J. Zhang, Discovery of novel anti-angiogenesis agents. Part 8: diaryl thiourea bearing 1H-indazole-3-amine as multi-target RTKs inhibitors, *Eur. J. Med. Chem.* 141 (2017) 373–385.
- [30] X. Jiang, H. Liu, Z. Song, X. Peng, Y. Ji, Q. Yao, M. Geng, J. Ai, A. Zhang, Discovery and SAR study of c-Met kinase inhibitors bearing an 3-amino-benzo[d]isoxazole or 3-aminoindazole scaffold, *Bioorg. Med. Chem.* 23 (2015) 564–578.
- [31] Y. Shan, J. Dong, X. Pan, L. Zhang, J. Zhang, Y. Dong, M. Wang, Expanding the structural diversity of Bcr-Abl inhibitors: dibenzoylpiperazin incorporated with 1H-indazol-3-amine, *Eur. J. Med. Chem.* 104 (2015) 139–147.
- [32] A.K. El-Damasy, N.C. Cho, S.B. Kang, A.N. Pae, G. Keum, ABL kinase inhibitory and antiproliferative activity of novel picolinamide based benzothiazoles, *Bioorg. Med. Chem. Lett.* 25 (2015) 2162–2168.
- [33] A.K. El-Damasy, N.C. Cho, G. Nam, A.N. Pae, G. Keum, Discovery of a nanomolar multikinase inhibitor (KST016366): a new benzothiazole derivative with remarkable broad-spectrum antiproliferative activity, *ChemMedChem* 11 (2016) 1587–1595.
- [34] Reaction Biology corporation, Available from, http://www.reactionbiology.com/webapps/site/Kinase_Assay_Protocol.aspx. (Accessed 2 June 2020).
- [35] C.E. Carow, M. Levenstein, S.H. Kaufmann, J. Chen, S. Amin, P. Rockwell, L. Witte, M.J. Borowitz, C.I. Civin, D. Small, Expression of the hematopoietic growth factor receptor FLT3 (STK-1/Flk2) in human leukemias, *Blood* 87 (1996) 1089–1096.
- [36] F. Birg, N. Carbuca, O. Rosnet, D. Birnbaum, The expression of FMS, KIT and FLT3 in hematopoietic malignancies, *Leuk. Lymphoma* 13 (1994) 223–227.
- [37] W. Voigt, Sulforhodamine B Assay and Chemosensitivity, Chemosensitivity, Humana Press, 2005, pp. 39–48.
- [38] <http://www.reactionbiology.com/webapps/site/Target-Engagement-Assays.aspx>. (Accessed 2 June 2020).
- [39] L. Kiss, P.B. Bennett, V.N. Uebele, K.S. Koblan, S.A. Kane, B. Neagle, K. Schroeder, High throughput ion-channel pharmacology: planar-array-based voltage clamp, *Assay Drug Dev. Technol.* 1 (2003) 127–135.
- [40] M.C. Sanguinetti, M. Tristani-Firouzi, hERG potassium channels and cardiac arrhythmia, *Nature* 440 (2006) 463–469.
- [41] A.K. El-Damasy, J.H. Lee, S.H. Seo, N.C. Cho, A.N. Pae, G. Keum, Design and synthesis of new potent anticancer benzothiazole amides and ureas featuring pyridylamide moiety and possessing dual B-Raf(V600E) and C-Raf kinase inhibitory activities, *Eur. J. Med. Chem.* 115 (2016) 201–216.
- [42] DTP Human Tumor Cell Line Screen Process, 2020. Available from, https://dtp.cancer.gov/discovery_development/nci-60/methodology.htm. (Accessed 2 June 2020).
- [43] Dassault Systèmes BIOVIA, Discovery Studio Modeling Envi-Ronment, Dassault Systèmes, San Diego, 2016. Release 4. 5 (Version).